Pyrrolo[1,3]benzothiazepine-Based Atypical Antipsychotic Agents. Synthesis, Structure−Activity Relationship, Molecular Modeling, and Biological Studies

Giuseppe Campiani,*,[†] Stefania Butini,[†] Sandra Gemma,[†] Vito Nacci,[†] Caterina Fattorusso,[‡] Bruno Catalanotti,[§] Gianluca Giorgi,[||] Alfredo Cagnotto,[⊥] Mara Goegan,[⊥] Tiziana Mennini,[⊥] Patrizia Minetti,[#] M. Assunta Di Cesare,[#] Domenico Mastroianni,[#] Nazzareno Scafetta,[#] Bruno Galletti,[#] M. Antonietta Stasi,[#] Massimo Castorina,[#] Licia Pacifici,[#] Orlando Ghirardi,[#] Ornella Tinti,[#] and Paolo Carminati[#]

Dipartimento Farmaco Chimico Tecnologico, Università degli Studi di Siena, Via Aldo Moro, 53100 Siena, Italy, Dipartimento di Chimica delle Sostanze Naturali, Università degli Studi di Napoli Federico II, via D. Montesano 49, 80131 Napoli, Italy, Dipartimento di Scienze Farmaceutiche, Università degli Studi di Salerno, Via Ponte Don Melillo 11C, 84084 Fisciano, Italy, Centro Interdipartimentale di Analisi e Determinazioni Strutturali (CIADS), via Aldo Moro, Università degli Studi di Siena, 53100 Siena, Italy, Istituto di Ricerche Farmacologiche Mario Negri, Via Eritrea 62, 20157 Milano, Italy, and Sigma-Tau Industrie Farmaceutiche Riunite spa, Via Pontina Km 30,400, 00040 Pomezia, Italy

The prototypical dopamine and serotonin antagonist (±)-7-chloro-9-(4-methylpiperazin-1-yl)-9,10-dihydropyrrolo[2,1-*b*][1,3]benzothiazepine (**5**) was resolved into its *R* and *S* enantiomers via crystallization of the diastereomeric tartaric acid salts. Binding studies confirmed that the (*R*)-(−)-enantiomer is a more potent D_2 receptor antagonist than the (*S*)-(+)-enantiomer, with almost identical affinity at the 5-HT_2 receptor ((*S*)-(+)-**5**, log Y = 4.7; (*R*)-(−)-**5**, log Y = 7.4). These data demonstrated a significant stereoselective interaction of **5** at D_2 receptors. Furthermore, enantiomer (*S*)-(+)-**5** (ST1460) was tested on a panel of receptors; this compound showed an intriguing binding profile characterized by high affinity for H_1 and the α_1 receptor, a moderate affinity for α_2 and D_3 receptors, and low affinity for muscarinic receptors. Pharmacological and biochemical investigation confirmed an atypical pharmacological profile for (*S*)-(+)-**5**. This atypical antipsychotic lead has low propensity to induce catalepsy in rat. It has minimal effect on serum prolactin levels, and it has been selected for further pharmacological studies. (*S*)-(+)-**5** increases the extracellular levels of dopamine in the rat striatum after subcutaneous administration. By use of **5** as the lead compound, a novel series of potential atypical antipsychotics has been developed, some of them being characterized by a stereoselective interaction at D_2 receptors. A number of structure−activity relationships trends have been identified, and a possible explanation is advanced in order to account for the observed stereoselectivity of the enantiomer of (±)-**5** for D_2 receptors. The molecular structure determination of the enantiomers of **5** by X-ray diffraction and molecular modeling is reported.

Introduction

Schizophrenia is one of the major neuropsychiatric disorders characterized by a severe and chronic mental impairment.[1] For decades, neuroleptic drugs have been established as the treatment of choice for acute and chronic schizophrenia. Chlorpromazine and haloperidol (**1**; Chart 1) are representative of these classical (typical) antipsychotics. The fact that the therapeutic potency of typical antipsychotic drugs directly correlates with their affinity for dopamine D_2 receptors has been an important basis for the dopamine hypothesis of schizophrenia,[2] especially in light of the fact that dopamine antagonists (neuroleptics) are still the only established pharmacotherapy for psychosis.[3] While typical neuroleptic drugs are effective against the positive symptoms of psychosis such as hallucination and delusions, negative symptoms such as blunted affect, emotional with-drawal, cognitive deficits, apathy and motor retardation remain uncontrolled with these therapeutics for most schizophrenic patients.

The dopamine hypothesis of schizophrenia has been, however, profoundly challenged by clozapine (**2**; Chart 1), an atypical antipsychotic drug that differs from typical antipsychotics in its pharmacological, biochemical, and clinical profile.[3] With respect to classical neuroleptics, clozapine shows significantly greater efficacy, including an improved effect on negative symptoms, and causes a marked increase in dopamine output in the prefrontal cortex. This latter is of considerable interest because of the role of the prefrontal dopaminergic system in cognitive functions. This activity has been related to clozapine α_2 receptor occupancy, an interaction that could augment its clinical efficacy, while its α_1 blocking activity may protect against dopamine deficits.[3,4] In humans clozapine does not produce extrapiramidal side effects (EPS) (favorable 5-HT_2/D_2 affinity ratio[5]) and it does not elevate prolactin serum levels. In rodents it does not induce catalepsy. However, occurrence of agranulocytosis in 0.6% of patients during treatment has been claimed.[6−8] Another recently marketed atypical antipsychotic drug is olanzapine (**3**; Chart

* To whom correspondence should be addressed. Phone: 0039-0577-234172. Fax: 0039-0577-234333. E-mail:campiani@unisi.it.
† Università degli Studi di Siena.
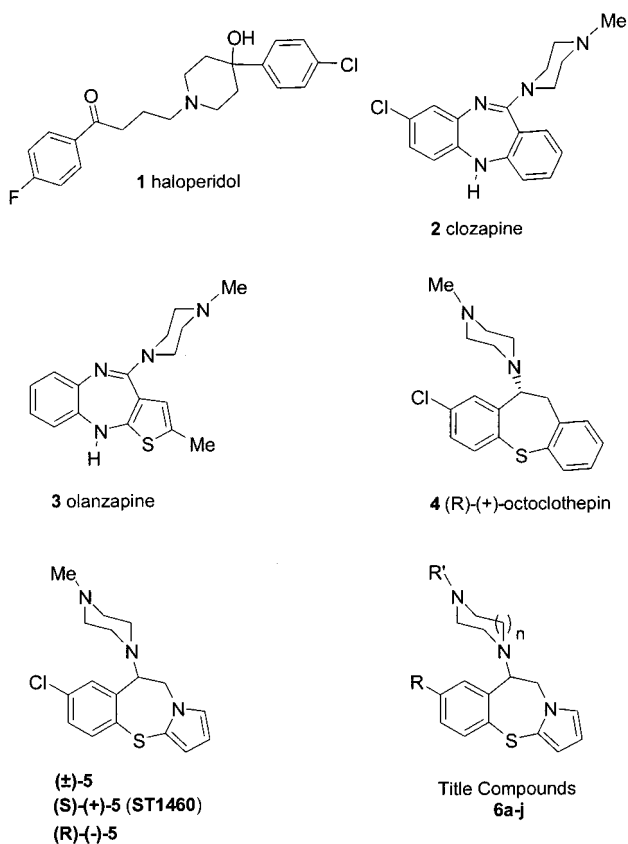‡ Università degli Studi di Napoli "Federico II".
§ Università degli Studi di Salerno.
|| CIADS, Università degli Studi di Siena.
⊥ Istituto di Ricerche Farmacologiche Mario Negri.
# Sigma-Tau Industrie Farmaceutiche Riunite.

Chart 1

1 haloperidol

2 clozapine

3 olanzapine

4 (R)-(+)-octoclothepin

(±)-**5**
(S)-(+)-**5** (ST1460)
(R)-(−)-**5**

Title Compounds
6a-j

Scheme 1

1).[9,10] The binding profile of olanzapine is similar to that of clozapine although it shows higher affinity for dopaminergic and 5-HT$_{2A}$ receptors and a lower affinity for α_1 and α_2 receptors.[11] Although it shows a binding profile similar to that of **2**, only one case of agranulocytosis has been reported with the clinical use of olanzapine.[12] The differences in covalent binding exhibited by the metabolites related to the two compounds, and in particular, the lack of olanzapine binding to human neutrophils in vivo may help to explain the difference in toxicity of these two drugs.[13,14] The intriguing pharmacological profile of these compounds has been called "atypical", and now clozapine and olanzapine represent the standard neuroleptics to which the new antipsychotic agents are compared. All these considerations prompted us to develop a project aimed at identifying novel atypical antipsychotic compounds based on a tricyclic skeleton. Recently we described prototypical dopamine/serotonin receptor antagonists[15] structurally related to octoclothepin **4** (Chart 1), a neuroleptic characterized by a rather low stereoselectivity at D$_2$ receptor whose (R)-(−)-enantiomer showed a more atypical binding profile.[16] In particular, the structure of octoclothepin was modified by replacing a benzo-fused ring with a pyrrole, and (±)-7-chloro-9-(4-methylpiperazin-1-yl)-9,10-dihydropyrrolo[2,1-*b*][1,3]-benzothiazepine (±)-**5** (Chart 1) was identified as the lead compound.[15] In this work we report the pharmacological and biochemical characterization of the (S)-(+)-**5** (ST1460) as a new atypical antipsychotic agent, and the synthesis, biological characterization, and structure−activity relationships of novel potential antipsychotics with clozapine- and olanzapine-like properties. A comprehensive study using X-ray diffraction and
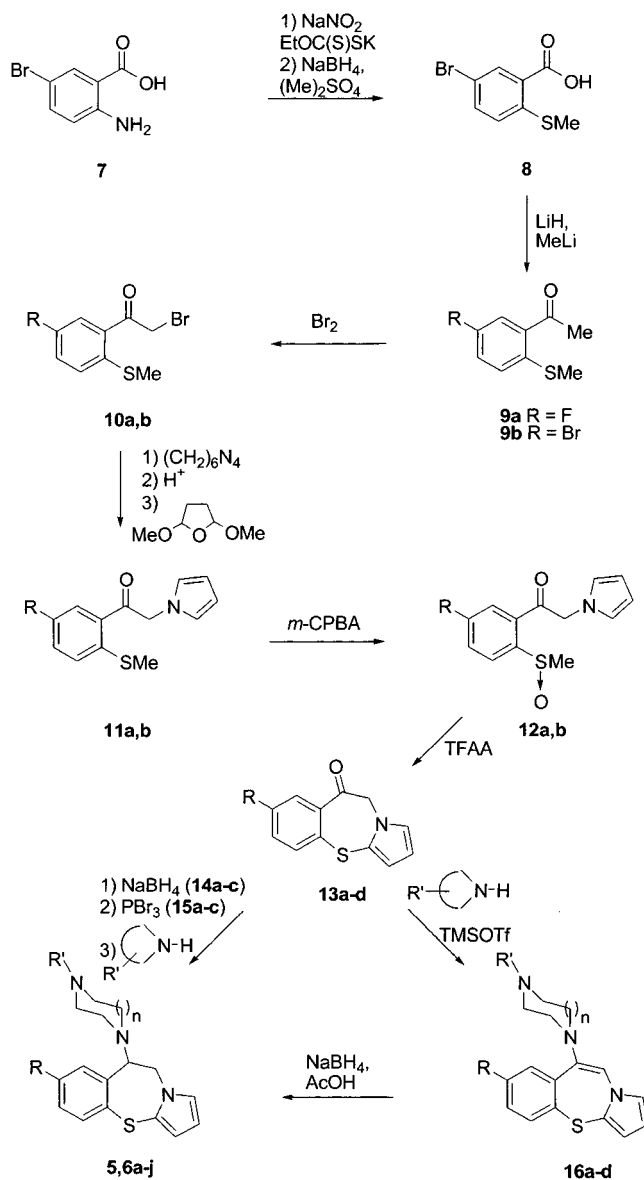
molecular modeling was performed in order to determine the conformational properties and the mutual orientation of the D$_2$ pharmacophoric features of (S)-(+)-**5**. Additionally, a molecular modeling approach to account for the observed stereoselectivity of both enantiomers of **5** at the D$_2$ receptor will be discussed.

Chemistry

The synthesis of the pyrrolo[2,1-*b*][1,3]benzothiazepine skeleton was accomplished as described in Scheme 1.[15] The key intermediates **10a,b** (R = F, Br) were prepared by bromination of the corresponding phenylethanones **9a,b**.[17] Compound **9a** was prepared from 1-fluoro-4-(methylthio)benzene by a standard Friedel−Crafts reaction with acetic anhydride, and **9b** was prepared by the reaction of methyllithium with the lithium salt of 5-bromo-2-(methylthio)benzoic acid **8** (Scheme 1). Benzoic acid **8** was synthesized from 2-amino-5-bromobenzoic acid **7** by a Sandmeyer-type reaction followed by sodium borohydride reduction of the disulfide intermediate and subsequent methylation (dimethyl sulfate). Subsequently, the bromophenylethanones **10a,b** were
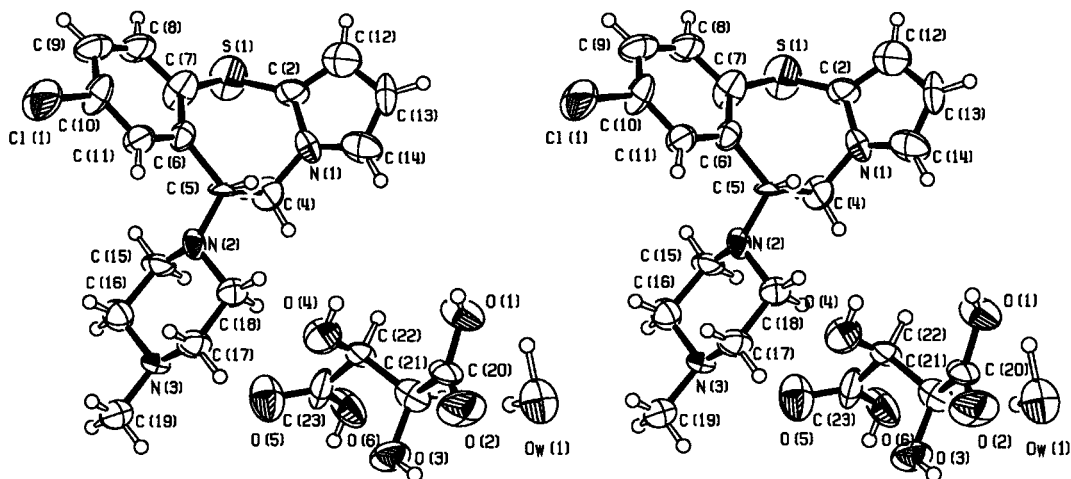
Figure 1. Stereodrawing of compound (*R*)-(−)-**5** tartrate·H_2O with the labeling of the atoms. The non-H-atom ellipsoids enclose 50% probability.

transformed into pyrrole derivatives **11a**,**b** by the Delepine reaction[18] followed by the Clauson−Kaas reaction.[19] Oxidation with *m*-chloroperbenzoic acid (*m*-CPBA) (**12a**,**b**) followed by exposure of these sulfoxides to trifluoroacetic anhydride provided the ketones **13a**,**b** in 69% yield. The "interrupted" Pummerer rearrangement begins with the activation of the sulfoxide oxygen followed by the attack of the pyrrole ring on sulfur, displacing the trifluoroacetate ion. Then the sulfonium salt undergoes displacement of the methyl group, generating the heterocyclic system and methyl trifluoroacetate.[20] Starting from the newly synthesized ketones **13a**,**b** and from the previously synthesized ketones **13c**,**d** (R = Cl, H), the piperazine ring was introduced following two different pathways. Accordingly, reduction of ketones **13a**−**c** (R = F, Br, Cl) provided the alcohols (±)-**14a**−**c**, which were transformed into the bromo derivatives (±)-**15a**−**c** by means of PBr_3. By treatment of (±)-**15a**−**c** with *N*-alkylpiperazine, the final products (±)-**6b**,**d**,**f**,**g**,**j** (Chart 1) were obtained.[21] On the other hand, following a different strategy, the enamines (±)-**16a**−**d** were prepared from **13b**−**d** by reaction with *N*-alkylpiperazines and *N*-methylhomopiperazine in the presence of trimethylsilyl triflate (TMSOTf). Sodium borohydride reduction of the double bond of **16a**−**d** provided compounds (±)-**6c**,**e**,**h**,**i**. Compounds (±)-**5** and (±)-**6a** were resynthesized following this latter strategy.

The thiazepine (±)-**5** was resolved by HPLC in the enantiomers (+)-**5** and (−)-**5** using a Chiralpak AD amylose column[15] or via the diastereomeric tartaric acid salts, and the stereochemistry of (−)-**5** tartaric acid salt was assigned by X-ray analysis (Figure 1). Compounds (±)-**6a** and (±)-**6b** were resolved into the enantiomers (+)-**6a** and (−)-**6a** and into (+)-**6b** and (−)-**6b**, respectively, via the diastereomeric tartaric acid salts.

Results and Discussion

Physical and chemical data for **5**, **6a**−**j**, and **16a**−**d** are shown in Table 1. The binding affinities for 5-HT_{2A}, D_1, D_2, and D_3 receptors and a comparison of pK_i values and log *Y* scores[22] of compounds **5** and **6**, together with clozapine, olanzapine, and haloperidol, tested under the same experimental conditions, are given in Tables 2 and 3. Table 4 summarizes the binding affinity of a subset of compounds for a panel of different receptors. Effects
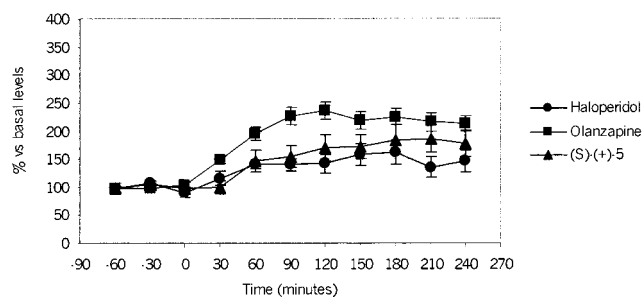

Figure 2. Effect of sequential injections of (*S*)-(+)-**5** at two doses (7.4 μmol/kg; 24.8 μmol/kg, sc), olanzapine (7.4 μmol/kg; 24.8 μmol/kg, sc), and haloperidol (0.74 μmol/kg; 7.4 μmol/kg, sc) on the dopamine levels in the dialysates obtained from rat striatum.

Figure 3. Effect of sequential injections of (*S*)-(+)-**5** at two doses (7.4 μmol/kg; 24.8 μmol/kg, sc), olanzapine (7.4 μmol/kg; 24.8 μmol/kg, sc), and haloperidol (0.74 μmol/kg; 7.4 μmol/kg, sc) on the DOPAC levels in the dialysates obtained from rat striatum.
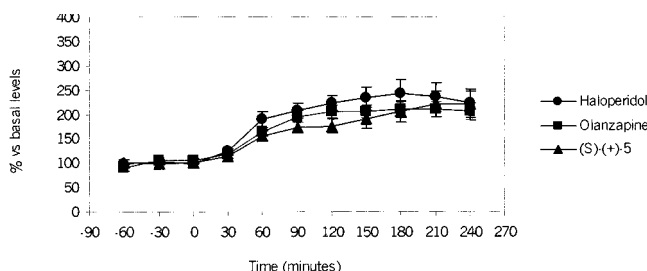
of (+)-**5** and (+)-**6a** on catalepsy, apomorphine climbing, and 5-MeO-DMT-induced head twitches, after oral and subcutaneous (sc) administration, compared to the effects of olanzapine and clozapine are shown in Table 5. The capability of (*S*)-(+)-**5** to increase the extracellular levels of dopamine, of 3,4-dihydroxyphenylacetic acid (DOPAC), and of homovanillic acid (HVA) in the striatum compared to the corresponding effects of haloperidol and olanzapine are reported in Tables 6 and 7 and Figures 2−4, while alterations of prolactin serum levels (PRL) induced by (*S*)-(+)-**5**, clozapine, olanzapine, and haloperidol are compared in Figure 5.

Pharmacological Studies. 1. (*S*)-(+)-5 (ST1460): A New Atypical Antipsychotic Agent. Binding Assays. Compound (±)-**5** was selected as the lead

Table 1. Physical and Chemical Data for Compounds **5**, **6a–j** and **16a–d**

compd	R	n	R′	yield[a] (%)	mp (°C)	recryst solvent[b]	formula	anal.[c]
(+)-**5** (ST1460)	Cl	1	Me				$C_{17}H_{20}ClN_3S$	C, H, N
(−)-**5**	Cl	1	Me				$C_{17}H_{20}ClN_3S$	C, H, N
(±)-**6a**[d]	H	1	Me				$C_{17}H_{21}N_3S$	C, H, N
(+)-**6a** (ST1622)	H	1	Me			A	$C_{17}H_{21}N_3S$	C, H, N
(−)-**6a**	H	1	Me			A	$C_{17}H_{21}N_3S$	C, H, N
(±)-**6b**	F	1	Me	63	213–214	B	$C_{17}H_{20}FN_3S$	C, H, N
(+)-**6b** (ST1615)	F	1	Me				$C_{17}H_{20}FN_3S$	C, H, N
(−)-**6b**	F	1	Me				$C_{17}H_{20}FN_3S$	C, H, N
(±)-**6c**	Cl	1	Et	84	207–208	A	$C_{18}H_{22}ClN_3S$	C, H, N
(±)-**6d**	Cl	1	CH_2CH_2OH	82	oil		$C_{18}H_{22}ClN_3OS$	C, H, N
(±)-**6e**	Cl	2	Me	59	oil		$C_{18}H_{22}ClN_3S$	C, H, N
(±)-**6f**	F	1	Et	73	oil		$C_{18}H_{22}FN_3S$	C, H, N
(±)-**6g**	F	1	CH_2CH_2OH	69	amorphous		$C_{18}H_{22}FN_3OS$	C, H, N
(±)-**6h**	Br	1	Me	79	amorphous		$C_{17}H_{20}BrN_3S$	C, H, N
(±)-**6i**	Br	1	Et	76	203–204	B	$C_{18}H_{22}BrN_3S$	C, H, N
(±)-**6j**	Br	1	CH_2CH_2OH	22	oil		$C_{18}H_{22}BrN_3OS$	C, H, N
16a	Cl	2	Me	41	123–125	C	$C_{18}H_{20}ClN_3S$	C, H, N
16b	Cl	1	Et	74	116–117	B	$C_{18}H_{20}ClN_3S$	C, H, N
16c	Br	1	Me	84	120–122	B	$C_{17}H_{18}BrN_3S$	C, H, N
16d	Br	1	Et	94	133–135	B	$C_{18}H_{20}BrN_3S$	C, H, N

[a] Yields refer to isolated and purified materials. [b] A = hexanes; B = hexanes/EtOAc, 3:1; C = EtOAc. [c] All the compounds were analyzed to within ±0.4% of the theoretical values. [d] From ref 15.
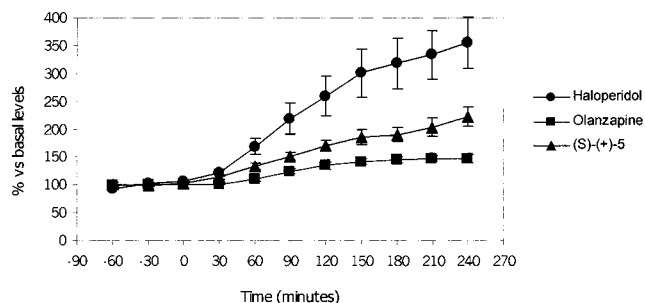

Figure 4. Effect of sequential injections of (*S*)-(+)-**5** at two doses (7.4 μmol/kg; 24.8 μmol/kg, sc), olanzapine (7.4 μmol/kg; 24.8 μmol/kg, sc), and haloperidol (0.74 μmol/kg; 7.4 μmol/kg, sc) on the HVA levels in the dialysates obtained from rat striatum.

compound of the new series, and the binding profile of its enantiomers was reinvestigated. An in-depth phar-

macological investigation of its enantiomers, initially separated by HPLC and then separated via the diastereomeric tartaric acid salt, brought to light the atypical binding profile of the (+)-enantiomer ((*S*)-(+)-**5**) and a typical binding profile of the (−)-enantiomer ((*R*)-(−)-**5**) (Tables 2 and 3). This latter is characterized by higher affinity for D_2 receptor similar to that for $5\text{-}HT_{2A}$ receptor. Conversely, as shown in Table 3, (+)-**5** (log Y = 4.7) displayed a binding profile similar to that of olanzapine (log Y = 4.7), and in particular, (+)-**5** was characterized by high affinity for the $5\text{-}HT_{2A}$ receptor, a significant affinity for D_1 and H_1 receptors, and a lower affinity for D_2, D_3, and muscarinic receptors (Tables 3 and 4). Serotonin (5-HT) via the stimulation of $5\text{-}HT_2$ receptor inhibits neuronal activity in the substantia nigra (SN) and ventral tegmental area (VTA).[23,24] Several studies have demonstrated that $5\text{-}HT_2$ antagonists increase the firing rate of midbrain
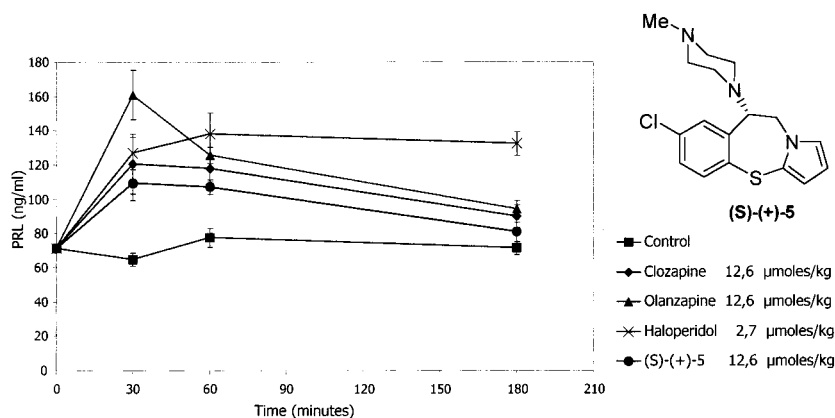

Figure 5. Time course for typical and atypical antipsychotic agents induced increases in serum prolactin levels (PRL). Effect of (*S*)-(+)-**5** is shown.

Table 2. Binding Affinities for 5-HT$_{2A}$, D$_1$, D$_2$, and D$_3$ Receptors of Compounds **5** and **6**

compd	K_i ($\pm$SD)^a (nM)			
	5-HT$_{2A}$	D$_1$	D$_2$	D$_3$
($\pm$)-**5**	1.14 $\pm$ 0.12	27 $\pm$ 1.0	3.8 $\pm$ 0.5	4.1 $\pm$ 1.5
(S)-(+)-**5** (ST1460)	1.48 $\pm$ 0.20	16.4 $\pm$ 1.0	49.6 $\pm$ 6.0	110 $\pm$ 7.0
(R)-(−)-**5**	1.72 $\pm$ 0.25	22 $\pm$ 1.3	2.1 $\pm$ 1.3	1.85 $\pm$ 1.3
($\pm$)-**6a**	25 $\pm$ 4	216 $\pm$ 6	79 $\pm$ 7	103 $\pm$ 18
(S)-(+)-**6a** (ST1622)	17.5 $\pm$ 3	139 $\pm$ 12	601 $\pm$ 56	854 $\pm$ 116
(R)-(−)-**6a**	18 $\pm$ 1	159 $\pm$ 28	19 $\pm$ 2	23 $\pm$ 2
($\pm$)-**6b**	5.1 $\pm$ 0.40	51 $\pm$ 5.5	23.7 $\pm$ 2.2	19.4 $\pm$ 1.5
(S)-(+)-**6b** (ST1615)	3.5 $\pm$ 0.4	60 $\pm$ 8	245 $\pm$ 27	407 $\pm$ 92
(R)-(−)-**6b**	4.3 $\pm$ 0.8	63 $\pm$ 2	5.5 $\pm$ 0.1	9.3 $\pm$ 1.4
($\pm$)-**6c**	5.8 $\pm$ 0.7	18.2 $\pm$ 2.4	3.1 $\pm$ 0.3	4.5 $\pm$ 0.2
($\pm$)-**6d**	8.8 $\pm$ 0.5	27 $\pm$ 3	6 $\pm$ 1	3.6 $\pm$ 0.3
($\pm$)-**6e**	16 $\pm$ 2	53 $\pm$ 7	30 $\pm$ 4	58 $\pm$ 4
($\pm$)-**6f**	4.3 $\pm$ 0.52	31 $\pm$ 3.49	9.5 $\pm$ 0.83	18 $\pm$ 0.88
($\pm$)-**6g**	7.1 $\pm$ 0.61	72 $\pm$ 2.66	22 $\pm$ 3.77	13 $\pm$ 0.97
($\pm$)-**6h**	12 $\pm$ 1.25	14 $\pm$ 2.3	3.6 $\pm$ 0.2	3.6 $\pm$ 1.5
($\pm$)-**6i**	23 $\pm$ 3.4	14 $\pm$ 3.5	4 $\pm$ 0.25	7.4 $\pm$ 1.7
($\pm$)-**6j**	23 $\pm$3.4	20 $\pm$ 4.2	5 $\pm$ 0.3	10 $\pm$ 1.1
($\pm$)-**4**	0.23 $\pm$ 0.03	2.3 $\pm$ 0.15	0.5 $\pm$ 0.06	2.4 $\pm$ 0.37
(R)-(+)-**4**	0.33 $\pm$ 0.03	2.0 $\pm$ 0.17	3.6 $\pm$ 0.46	21 $\pm$ 4.35
(S)-(−)-**4**	0.14 $\pm$ 0.01	1.9 $\pm$ 0.53	0.4 $\pm$ 0.04	0.4 $\pm$ 0.04
clozapine	10.0 $\pm$ 1	350 $\pm$ 35	250 $\pm$ 57	320 $\pm$ 45
olanzapine	4.0 $\pm$ 1	85 $\pm$ 3.5	69 $\pm$17	39 $\pm$ 5.91
haloperidol	164 $\pm$ 22	318 $\pm$ 59	4.8 $\pm$ 1	18 $\pm$ 1.5

^{a} Each value is the mean $\pm$ SD of three determinations and represent the concentration giving half-maximal inhibition of [^{3}H]Ketanserin (5-HT$_2$), [^{3}H]SCH 23390 (D$_1$), [^{3}H]Spiperone (D$_2$), and [^{3}H]-7-OH-DPAT (D$_3$) binding to rat tissue homogenate.

Table 3. pK_i Values of D$_1$, D$_2$, D$_3$, and 5-HT$_{2A}$ Receptor Binding Sites, Ratios for Compounds **5** and **6**, Octoclothepin (**4**), Clozapine (Atypical), Olanzapine (Atypical), Haloperidol (Typical), and Methiothepin (Typical), and Their log Y Scores^a

compd	pK_i				5-HT$_{2A}$/D$_2$	D$_1$/D$_2$	D$_3$/D$_1$	log Y
	5-HT$_{2A}$	D$_1$	D$_2$	D$_3$				
($\pm$)-**5**	8.94	7.57	8.42	8.40	1.06	0.90	1.11	6.56
(S)-(+)-**5** (ST1460)	8.83	7.79	7.30	6.96	1.21	1.07	0.89	4.67
(R)-(−)-**5**	8.76	7.66	8.69	8.73	1.01	0.88	1.14	7.40
($\pm$)-**6a**	7.60	6.67	7.10	6.99	1.07	0.94	1.05	5.59
(S)-(+)-**6a** (ST1622)	7.76	6.86	6.22	6.07	1.25	1.10	0.89	3.73
(R)-(−)-**6a**	7.74	6.80	7.72	7.64	1.00	0.88	1.12	6.65
($\pm$)-**6b**	8.29	7.29	7.63	7.61	1.09	0.96	1.06	5.87
(S)-(+)-**6b** (ST1615)	8.46	7.22	6.61	6.39	1.28	1.09	0.88	3.60
(R)-(−)-**6b**	8.37	7.20	8.26	8.03	1.01	0.87	1.12	6.95
($\pm$)-**6c**	8.23	7.74	8.51	8.35	0.97	0.91	1.08	7.93
($\pm$)-**6d**	8.06	7.57	8.23	8.44	0.98	0.92	1.11	7.56
($\pm$)-**6e**	7.27	7.27	7.53	7.24	0.96	0.97	0.99	7.25
($\pm$)-**6f**	8.36	7.51	8.02	7.74	1.04	0.94	1.03	6.95
($\pm$)-**6g**	7.13	7.14	7.66	7.88	1.06	0.93	1.10	6.08
($\pm$)-**6h**	7.92	7.84	8.44	8.44	0.94	0.93	1.08	8.33
($\pm$)-**6i**	7.64	7.85	8.40	8.13	0.91	0.94	1.04	8.68
($\pm$)-**6j**	7.65	7.70	8.30	8.00	0.92	0.93	1.04	8.40
($\pm$)-**4**	9.64	8.64	9.30	8.62	1.04	0.93	1.00	7.77
(R)-(+)-**4**	9.48	8.69	8.44	7.68	1.12	1.03	0.88	6.35
(S)-(−)-**4**	9.85	8.71	9.40	9.38	1.05	0.93	1.08	7.66
clozapine	8.00	6.45	6.60	6.50	1.21	0.98	1.01	3.89
olanzapine	8.40	7.07	7.16	7.41	1.17	0.99	1.05	4.69
haloperidol	6.78	6.50	8.32	7.74	0.82	0.78	1.19	9.14
methiothepine^b	9.40	8.70	9.40		0.97	0.90		8.95

^{a} The log Y score has been calculated according to the equation reported in ref 22. The cutoff point is 6.48. The equation used to calculate the log Y score is log $Y = (0.52)(pK_i\ D_1) + (1.952)(pK_i\ D_2) - (1.544)(pK_i\ 5\text{-HT}_{2A})$. ^{b} Data from ref 22.

dopaminergic neurons in state-dependent manner. 5-HT$_{2A}$ antagonists, although devoid of effects by themselves, have been shown to potentiate the increase in the activity of nigrostriatal DA-containing neurons that occur in response to the moderate D$_2$ receptor blockade by antipsychotic drugs.[25] So, 5-HT$_{2A}$ antagonists may prevent or alleviate extrapyramidal symptoms (EPS) induced by acute or long-term treatment with typical neuroleptics (haloperidol) through their modulatory influence on nigrostriatal dopaminergic transmission.[26−30] Thus, the favorable 5-HT$_{2A}$/D$_2$ affinity ratio of (S)-(+)-**5** may greatly contribute to the atypical profile and efficacy of this new antipsychotic agent (see Behavioral

and Biochemical Effects). A critical aspect of the clozapine binding profile is its affinity for α receptors.[4a,b] The α_2 receptor occupancy could explain the marked increase in dopamine output in the prefrontal cortex induced by clozapine, which is beneficial to cognitive functions. Accordingly, compound (S)-(+)-**5** shows a significant affinity for the α_2 receptor, similar to that of clozapine. This fact could augment the clinical efficacy of (S)-(+)-**5**, while its α_1 blocking activity may protect against dopamine deficits. Conversely, (−)-**5** is characterized by a nanomolar affinity for 5-HT$_{2A}$, D$_2$, and D$_3$ receptors, with lower affinity for the D$_1$ receptor (K_i = 22 nM). These data confirm the typical binding profile of (−)-**5**

Table 4. Binding Affinities for H_1, M_1, α_1, and α_2 Receptors of Compounds **5** and **6**

compd	K_i (±SD)[a] (nM)			
	H_1	M_1	α_1	α_2
(S)-(+)-**5** (ST1460)	21.3 ± 9.3	287 ± 13.3	0.82 ± 0.04	209 ± 20.9
(S)-(+)-**6a** (ST1622)	9.5 ± 2.51	2272 ± 118	18.8 ± 1.1	b
(S)-(+)-**6b** (ST1615)	33.0 ± 8.8	>10 000	12.0 ± 0.70	b
(R)-(−)-**6b**	4.6 ± 0.62	>10 000	4.5 ± 0.2	b
(±)-**6f**	4.3 ± 0.44	2344 ± 112	0.4 ± 0.01	b
(±)-**6g**	7.1 ± 0.08	6300 ± 212	2.9 ± 0.38	b
clozapine	14.0 ± 0.01	55 ± 0.001	8.9 ± 3.0	128 ± 9.3
olanzapine	0.35 ± 0.10	22.0 ± 13.1	14.6 ± 0.99	2870 ± 384
haloperidol	384 ± 0.01	>10 000	12 ± 2.5	2700 ± 242

[a] Each value is the mean ± SD of three determinations and represent the concentration giving half-maximal inhibition of [3H]Pirilamine (H_1), [3H]QNB (M), [3H]Prazosin (α_1), and [3H]Clonidine (α_2) binding to rat frontal cortex homogenate. [b] Not tested.

Table 5. In Vivo Effect on Serotoninergic and Dopaminergic Systems

		5-MeO-DMT-induced head twitches		apomorphine climbing		catalepsy induction	
		mg/kg	μmol/kg[a]	mg/kg	μmol/kg[a]	mg/kg	μmol/kg[a]
Clozapine	sc	0.33	1.01	0.93	2.86	c	
	os	c		c		c	
Olanzapine	sc	0.18	0.58	0.12	0.38	6.5	22
	os	1.45	4.65	2.69	8.61	21.2	67.9
(S)-(+)-**5**[b]	sc	0.19	0.48	0.10	0.24	18.3	45
	os	5.83	14.34	7.90	19.50	46.7	114.8
(S)-(+)-**6a**[b]	sc	0.83	2.8	1.5	5.2	>100	269
	os	c		c		c	

[a] ED50 values were calculated after subcutaneous or oral administration of the tested compounds. [b] (+)-**5** was used as the dihydrochloride salt, and (+)-**6a** was used as maleate salt. [c] Not tested.

(log Y = 7.4). The (±)-**5** unsubstituted counterpart (±)-**6a** was also resynthesized, and the racemate was resolved into the enantiomers (+)-**6a** (ST1622) and (−)-**6a** using HPLC techniques. Overall, (+)-**6a** was characterized by an atypical binding profile with a particularly favorable 5-HT$_{2A}$/D$_2$ affinity ratio (log Y = 3.7), although it is a less potent ligand than (+)-**5** for the panel of different receptors, while (−)-**6a** presented a typical binding profile (log Y = 6.65), as shown in Table 3.

These binding data pointed out a stereoselective interaction of both enantiomers of (±)-**5** and (±)-**6a** at the D$_2$ receptor, the (+)-enantiomers being 24-fold and 30-fold, respectively, less potent than the (−)-enantiomers. In the case of octoclothepin, the (R)-(−)- and the (S)-(+)-enantiomers bind the D$_2$ receptor with a rather low degree of stereoselectivity (9-fold). An approach to explain the stereoselective interaction at D$_2$ receptor of

the novel antipsychotics is discussed in the molecular modeling section.

2. Behavioral and Biochemical Effects: (+)-5 (ST1460) vs (+)-6a (ST1622). Tests were performed on the dihydrochloride salt of (S)-(+)-**5** and on the maleate salt of (S)-(+)-**6a**. Previously we reported that (±)-**5** at low doses did not induce extrapyramidal motor disturbances, displaying an atypical profile, but unlike olanzapine, at high doses it induced catalepsy. The separation between doses that suppressed apomorphine-induced locomotor activity and those inducing catalepsy indicated anyway a considerable safety margin for the induction of EPS in the racemate (±)-**5**. Furthermore, (±)-**5** (30 nmol/kg) elevated extracellular dopamine levels in striatum, while a smaller but significant increase in extracellular levels of DOPAC was observed. The racemate (±)-**5** has now been resolved, and the enantiomer (S)-(+)-**5** was pharmacologically characterized. As shown in Table 5, subcutaneous acute administration of (S)-(+)-**5** (18.3 mg/kg, 45 μmol/kg) induced catalepsy in 50% of the treated animals after 240 min of injection, whereas the maximal induction of catalepsy was measured after injection of 24.4 mg/kg (240 min). Olanzapine, tested under the same experimental conditions, induced catalepsy in 50% of the treated animals after 90 min from the sc administration of 7 mg/kg (22 μmol/kg), with a maximum effect at 9.4 mg/kg (180 min). Thus, (S)-(+)-**5** induces catalepsy to a lesser extent than olanzapine and does not induce extrapyramidal side effects at antipsychotic dosages. Similar results were found after oral administration. Furthermore, (S)-(+)-**5** effectively antagonizes 5-HT$_2$ receptors in vivo. After sc administration (6 min) of 5-MeO-DMT (5-methoxy-N,N-dimethyltriptamine) (10 mg/kg), the number of 5-MeO-DMT-induced head twitches was evaluated for a period of 15 min. (S)-(+)-**5** was administered orally or subcutaneously (60 or 30 min before 5-MeO-DMT, respectively), and data were compared to clozapine and olanzapine. After sc administration, (S)-(+)-**5** (ED50 = 0.48 μmol/kg) antagonized 5-MeO-DMT-induced head twitches at equimolar dose as olanzapine (ED50 = 0.58 μmol/kg), while to reach the same effect a higher dose (0.33 mg/kg, ED50 = 1.01 μmol/kg) of clozapine was necessary. On the other hand, after oral administration, (S)-(+)-**5** was found to be less potent than orally administered olanzapine (ED50 = 14.3 and 4.65 μmol/kg, respectively). (+)-**6a** (ST1622) was also tested under the same experimental conditions. After sc administration, (+)-**6a** demonstrated a lower potency (ED50 = 2.8 μmol/kg) than (S)-(+)-**5**, olanzapine, and, to a lower extent, clozapine (Table 5). The ability to antagonize apomorphine-induced climbing behavior in mice was also evaluated for (S)-(+)-**5** and (+)-**6a**. Subcutaneous

Table 6. Area under the Curve (AUC) Values of Dopamine, DOPAC, and HVA Extracellular Levels Accumulated in Dialysates Collected from Rat Striatum after the Sequential Treatment, Showing Effect of (S)-(+)-**5** at Two Doses

compd	AUC[c] first treatment			AUC[c] second treatment			AUCtot[c]		
	DA	DOPAC	HVA	DA	DOPAC	HVA	DA	DOPAC	HVA
(S)-(+)-**5**[a]	133.6 ± 14.3[d]	145.4 ± 8.2	133.1 ± 4.5[d,e]	179.0 ± 23.2	203.5 ± 21.7	193.8 ± 14.2[d,f]	156.3 ± 18.4[g]	174.4 ± 14.8	163.4 ± 9.3[d,f]
olanzapine[a]	184.7 ± 8.8	157.7 ± 7.8	113.1 ± 2.8	220.8 ± 14.3	207.3 ± 14.6	143.7 ± 5.8	202.8 ± 11.4	182.5 ± 11.0	128.4 ± 4.2
haloperidol[b]	129.2 ± 7.1	170.6 ± 9.9	172.5 ± 29.2	149.7 ± 18.6	233.9 ± 24.2	315.2 ± 15.8	139.4 ± 12.3	202.9 ± 14.9	243.8 ± 29.2

[a] Tested at 7.4 μmol/kg (first treatment) and 24.8 μmol/kg (second treatment). [b] Tested at 0.74 μmol/kg (first treatment) and 7.4 μmol/kg (second treatment). [c] Data are the mean ± SEM. For (S)-(+)-**5**, olanzapine, and haloperidol: $n = 6$, $n = 7$, $n = 5$, respectively. [d] Student's t-test for unpaired data vs olanzapine: $p \leq 0.01$. [e] Student's t-test for unpaired data vs haloperidol: $p \leq 0.05$ [f] Student's t-test for unpaired data vs haloperidol: $p \leq 0.02$. [g] Student's t-test for unpaired data vs olanzapine: $p \leq 0.05$.

Table 7. Comparison of the Overall Effect of (S)-$(+)$-**5**, Olanzapine, and Haloperidol on Dopamine Release and Methabolism in Rat Striatum[a]

	DA/DOPAC	DA/HVA
(S)-$(+)$-**5** $(n=6)$	$0.90 \pm 0.07^{b,c}$	1.0 ± 0.16^{d}
olanzapine $(n = 7)$	1.12 ± 0.06	1.6 ± 0.1
haloperidol $(n = 5)$	0.7 ± 0.035	0.6 ± 0.06

[a] Data are the mean $\pm$ SEM. [b] Student's t-test for unpaired data vs olanzapine: $p < 0.05$. [c] Student's t-test for unpaired data vs haloperidol: $p < 0.05$. [d] Student's t-test for unpaired data vs olanzapine: $p < 0.01$.

administration of (S)-$(+)$-**5** prior to 1.3 mg/kg apomorphine caused a dose-related suppression of apomorphine-induced climbing (Table 5). The compound showed an ED_{50} (0.24 μmol/kg) similar to that of olanzapine $(ED_{50} = 0.38 \mu$mol/kg). At these doses, (S)-$(+)$-**5** did not induce catalepsy. In contrast, clozapine caused a dose-related suppression in apomorphine-induced climbing up to a dose of 2 μmol/kg $(ED_{50} = 2.86 \mu$mol/kg). After oral administration in mice, (S)-$(+)$-**5** $(ED_{50} = 19.5 \mu$mol/kg) was less potent than olanzapine $(ED_{50} = 8.6 \mu$mol/kg). Administration of $(+)$-**6a** (sc) to mice induced a dose-related suppression of apomorphine-induced climbing, although it showed a lower potency $(ED_{50} = 5.2 \mu$mol/kg) with respect to that of (S)-$(+)$-**5** and olanzapine. Even in this case, the dose that antagonized apomorphine-induced climbing was much lower than the dose that induced catalepsy $(>100$ mg/kg) (Table 5). In light of these results, (S)-$(+)$-**5** was selected for further studies.

As shown in Tables 6 and 7 and Figures 2−4, sc administration of haloperidol $(n = 5$; 0.74 and 7.4 μmol/kg), (S)-$(+)$-**5** $(n = 6$; 7.4 and 24.8 μmol/kg), and olanzapine $(n = 7$; 7.4 and 24.8 μmol/kg) induced an increase in extracellular DA levels of 139%, 156%, 202%, respectively. However, while haloperidol induced a greater increase of extracellular levels of DOPAC (202%) and HVA (243%) compared with DA levels, (S)-$(+)$-**5** was found to increase DA and DOPAC levels to about the same extent as olanzapine (Table 7, Figure 3). In the case of haloperidol, these neurochemical events may be related to the high D_2 receptor antagonism of the drug, while for (S)-$(+)$-**5**, as for olanzapine, these acute effects in the striatum may be induced by a serotoninergic modulating effect on DA nigrostriatal activity, related to the higher affinity for 5-HT$_2$ receptor compared to D_2 receptor, of the two antipsychotics. The tested compounds differentially affect dopamine release and metabolism in rat striatum in vivo. As shown in Table 7, by comparison of the dopamine/metabolites ratio for (S)-$(+)$-**5** and olanzapine (DA/DOPAC of 0.90 and 1.12, respectively, to haloperidol 0.69; DA/HVA of 0.98 and 1.59, respectively, to haloperidol 0.59), it is clearly evident that (S)-$(+)$-**5** and olanzapine elevate the dopamine synthesis/release and metabolism to approximately the same degree, while haloperidol induces a more pronounced increase of dopamine metabolism in the striatum. So, the favorable 5-HT$_{2A}$/D$_2$ affinity ratio of these two antipsychotics may account for the low induction of extrapyramidal motor disturbances induced by atypical antipsychotics. Furthermore, administration of 12.6 μmol/kg (sc) of (S)-$(+)$-**5** induced an increase of prolactin serum levels (PRL) lower than clozapine, olanzapine (tested at the same dose), and the typical neuroleptic haloperidol (2.7 μmol/kg) (Figure 5).[31]

3. Novel (S)-$(+)$-5 Analogues. Binding Studies. (S)-$(+)$-**5** has been characterized as a novel atypical antipsychotic. While further pharmacological studies are in progress to assess its potential effect as a new drug (preclinical studies), a series of novel analogues based on the pyrrolo[1,3]benzothiazepine skeleton were developed. We report herein the pharmacological characterization (Table 3) of new analogues of (S)-$(+)$-**5**, in which the chlorine atom has been replaced by a fluorine or by a bromine atom, and of derivatives in which the piperazine ring has been differently alkylated. As shown in Table 3, $(\pm)$-**6b** showed a favorable log Y score (5.9), while its corresponding bromo analogue $(\pm)$-**6h** presented a log Y score (8.3) similar to those of typical neuroleptics. Binding studies (5-HT$_{2A}$, D$_1$, D$_2$, and D$_3$ receptors) performed on $(\pm)$-**6a,b,h** and compared to the study of $(\pm)$-**5** show that substitution of the benzo-fused ring at position 7 with chlorine and, to a lesser extent, fluorine is critical for the potency of binding to serotonin and dopamine receptors. Overall, $(\pm)$-**5** and $(\pm)$-**6b** display a higher affinity for serotonin and dopamine receptors than $(\pm)$-**6a**. Analogue $(\pm)$-**6b** shows a lower potency of binding to dopamine receptors than $(\pm)$-**5**, and it presents, already in the racemate form, a favorable log Y score (5.87). In contrast, the bromine atom of $(\pm)$-**6h** is well tolerated at dopamine receptors while it confers a slightly lower affinity to the 5-HT$_{2A}$ receptor. In fact it shows a log Y score equal to 8.33, similar to that of haloperidol (9.14). Accordingly, $(\pm)$-**6a,b** have been resolved into the enantiomers $(+)$-**6a,b** and $(-)$-**6a,b** and they were compared to those of $(\pm)$-**5**. In all cases the enantiomers show a different binding profile at 5-HT$_{2A}$ and D$_2$ receptors. In fact, $(-)$-**6b** and $(-)$-**6a** show a typical binding profile, being equipotent at 5-HT$_{2A}$ and D$_2$ receptors, while $(+)$-**6b** and $(+)$-**6a** represent new atypical agents characterized by a highly favorable 5-HT$_{2A}$/D$_2$ affinity ratio with a log Y score similar to that of clozapine (3.60 and 3.73, respectively; Table 3). Despite the fact that $(+)$- and $(-)$-octoclothepin enantiomers show a 9-fold stereoselectivity at D$_2$ receptors,[16] $(+)$-**5**, $(+)$-**6a**, and $(+)$-**6b** are 25-, 30-, and 45-fold, respectively, less potent at the D$_2$ receptor than their corresponding $(-)$-enantiomers, confirming a significant stereoselective interaction at D$_2$ receptor. This stereoselectivity directly depends on the substituents on the benzo-fused ring (F > H > Cl). In the substituted analogues, the affinity for serotonin and dopamine receptors is also slightly influenced by the substituents at N-4 of the piperazine ring. In general, substitution of the N-4 methyl group with an ethyl $((\pm)$-**6c,f,i**) or a β-hydroxyethyl chain $((\pm)$-**6d,g,j**) slightly modifies the potency at the 5-HT$_{2A}$ receptor, being $(\pm)$-**6c,f,i** similarly potent to the corresponding methyl derivatives $(\pm)$-**5** and $(\pm)$-**6b,h**. Introduction of a hydroxy group on the β-carbon of the ethyl chain at N-4 leads to high-affinity analogues $((\pm)$-**6d,g,j**) for D$_2$ receptors, while a slightly lower affinity was found at the 5-HT$_{2A}$ receptor. Substitution of the 4-methylpiperazinyl group of $(\pm)$-**5** with a 4-methylhomopiperazinyl group $((\pm)$-**6e**) caused a slight drop in affinity for serotonin and dopamine receptors probably due to unfavorable steric interactions. Taking into account these data, the methyl group
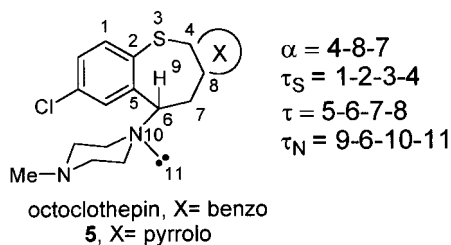
α = 4-8-7
τ_S = 1-2-3-4
τ = 5-6-7-8
τ_N = 9-6-10-11

octoclothepin, X= benzo
5, X= pyrrolo

Figure 6. Schematic displaying angle α and dihedral angles τ, τ_s, and τ_N for **5** and octoclothepin.

at N-4 of the piperazine ring seems to be optimal for a balanced interaction between serotonin and dopamine receptors.

Stereoselectivity at D$_2$ Receptors. Molecular Modeling Studies. Using molecular modeling techniques, we investigated the structural and conformational features responsible for increased stereoselectivity at D$_2$ receptors of (±)-**5** enantiomers with respect to those of (±)-octoclothepin.

The newly developed antipsychotic agent (S)-(+)-**5** shows an atypical binding profile in contrast to its (R)-(−)-enantiomer, which is typical. Binding studies results (Table 2) highlighted that a weaker interaction with the D$_2$ receptor binding site is a determinant for a favorable (S)-(+)-**5** 5-HT$_{2A}$/D$_2$ affinity ratio and atypical properties. Indeed, (R)-(−)-**5** binds the D$_2$ receptor with a 24-fold higher affinity than (S)-(+)-**5** ,while (S)-(−)-octoclothepin is only 9-fold more active than its (R)-(+)-enantiomer. The lack of significant stereoselectivity for octoclothepin enantiomers toward D$_2$ receptor has been explained by energetically allowed conformational changes of the tricyclic system, which enable both enantiomers to achieve the D$_2$ receptor bioactive conformation, fitting the proposed D$_2$ receptor pharmacophore.[16]

To explain reduced (S)-(+)-**5** D$_2$ receptor affinity, in the present study we investigated the role played by a pyrrolo ring (**5**) in place of the unsubstituted benzo-fused system of **4** in driving a change in the intramolecular forces of the tricyclic system, which could affect its capability to reach the proposed D$_2$ receptor bioactive conformation.[32] The correct orientation of the pharmacophoric groups (the substituted aromatic ring and the piperazine distal nitrogen) in the D$_2$ receptor binding site is mainly determined by rotation of internal torsion angles, defined in Figure 6. Rotation about the C−S−C bridge (τ_S, C_1−C_2−S_3−C_4) generates two different flips of the tricyclic system, while rotation about the C−C bonds in the ethylene bridge (τ, C_5−C_6−C_7−C/N$_8$) affects the mutual position of the substituted aromatic ring with respect to the distal protonatable nitrogen. On the other hand, the correct orientation of the distal nitrogen lone pair in the D$_2$ receptor binding site is given by the rotation around τ_N (H_9−C_6−N_{10}−LP_{11}) (proposed "bioactive" values for (S)-(−)- and (R)-(+)-octoclothepin are 172° and 325°, respectively[16]). By consequence, conformational changes leading to the bioactive conformation can be monitored through the variation of τ, τ_S, and τ_N torsion angles. Accordingly, energetic curves derived from the rotation about these angles were evaluated, for both (±)-octoclothepin and (±)-**5**, by means of systematic conformational search (Sybyl, Tripos, St. Louis, MO) and molecular mechanics (MM) calculations

Table 8. PM3 Calculated Energies and Corresponding Torsion Angles Values of (A) Octoclothepin and (±)-**5** Conformers and (B) Proposed Bioactive Conformations of Their Enantiomers

	E^a	τ^b	$\tau_S{}^b$	$\tau_N{}^b$
A. Conformers				
octoclothepin^c				
A	0.00	−82	−162	−48
B	0.05	−92	157	−171
C	0.78	56	130	−82
D	0.86	98	−140	−84
5^d				
A′	0.00	−90	180	−161
B′	2.24	85	−124	172
C′	2.83	56	133	−87
B. Bioactive Conformations				
(S)-(−)-octoclothepin	1.40	82	−125	172
(R)-(+)-octoclothepin	2.49	−38	−136	325
(R)-(−)-**5**	2.24	85	−124	172
(S)-(+)-**5**	5.06	−42	−120	325

^{a} ΔE from the lowest energy conformer. In units of kcal/mol. ^{b} Torsion angles as defined in Figure 6. Units in degrees. ^{c} Torsion angles values referenced to (S)-(−)octoclothepin. ^{d} Torsion angles values referenced to (R)-(−)-**5**.

(Discover, MSI San Diego). These preliminary results (data not shown) suggested a decreased capability for (S)-(+)-**5** to reach the D$_2$ receptor bioactive conformation compared to the capability of octoclothepin to adopt the corresponding (R)-(+)-enantiomer bioactive conformation. This conformational behavior could account for the different binding profiles found for the enantiomers of **5** and octoclothepin and for different stereoselectivity at D$_2$ receptor. To test this hypothesis, PM3 semiempirical calculations were performed on the MM resulting minima and then extended to the proposed D$_2$ receptor bioactive conformation of (S)-(−)- and (R)-(+)-octoclothepin as well as of (R)-(−)-**5** and (S)-(+)-**5**. Indeed, since enantiomers have identical physicochemical and thermodynamical properties, the difference in their free energy of binding to the D$_2$ receptor should largely be determined by the difference in the conformational energies of their biologically active conformations. In Table 8 are reported calculated PM3 energies and torsion angle values of the lowest energy minimum found for each conformational family of the tricyclic system calculated for (S)-(−)-octoclothepin and (R)-(−)-**5**, together with those calculated for the bioactive conformation of each enantiomer. Our results show that, as previously observed,[32] (R)-(+)-octoclothepin bioactive folding of the tricyclic system (conformer C in Table 8 and Figure 7) is slightly energetically favored with respect to the one of (S)-(−)-octoclothepin (conformer D in Table 8 and Figure 7). In contrast, (S)-(+)-**5** bioactive folding of the tricyclic system (C′ conformer in Table 8 and Figure 7) is energetically disfavored with respect to the one of (R)-(−)-**5** (B′ conformer in Table 8 and Figure 7). Nevertheless, aside from the folding of the tricyclic structure, the energy of the proposed D$_2$ bioactive conformation is also influenced by the pharmacophore required orientation of the distal piperazine nitrogen lone pair that is, in turn, determined by the rotation along τ_N. This conformational requirement is responsible for the higher energy of (R)-(+)-octoclothepin D$_2$ bioactive conformation with respect to the (S)-(−)-octoclothepin one, thus explaining the difference in the binding affinities of the two enantiomers ($K_{i(R)-(+)-\mathbf{4}}$ = 3.6 nM and $K_{i(S)-(−)-\mathbf{4}}$ = 0.4 nM). Accordingly, our
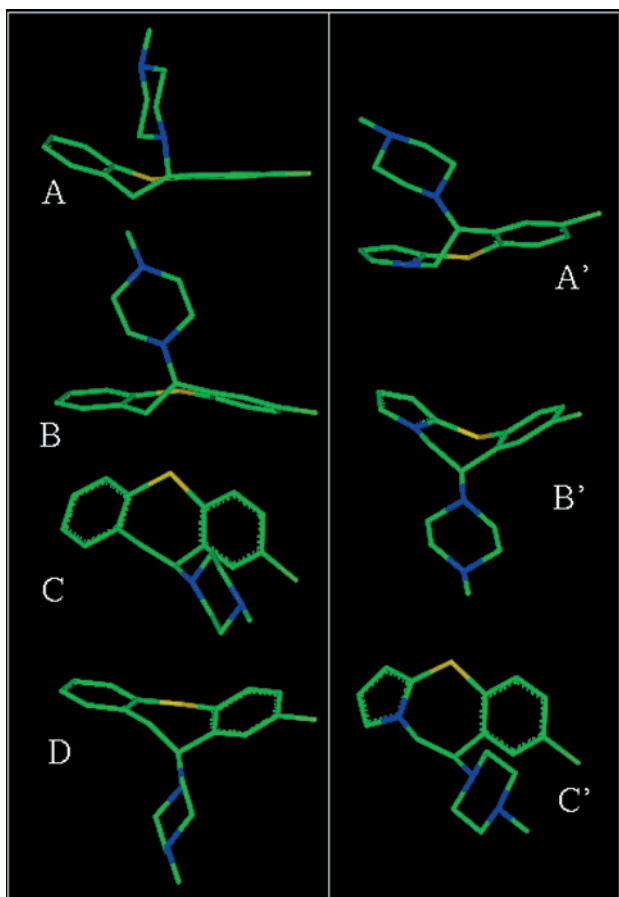
Figure 7. Octoclothepin (left) and **5** (right) resulting conformers sorted by descending energies and colored by atom type (sulfur = yellow, nitrogen = blue, chlorine = dark green). Hydrogens are omitted for clarity.

results show that (*S*)-(−)-octoclothepin bioactive conformation (conformer D with a τ_N value of 172°) is energetically favored ($\Delta E = -1.09$ kcal/mol) with respect to the bioactive conformation of (*R*)-(+)-octoclothepin (conformer C with a τ_N value of 325°). On the other hand, conformer B′ of (±)-**5** enantiomers corresponds to the bioactive flip of the (*R*)-(−)-enantiomer, and it is energetically favored with respect to conformer C′, which corresponds to the bioactive flip of the (*S*)-(+)-enantiomer. By consequence, taking into account the piperazine bioactive orientation ($\tau_N = 172°$ and 325° for (*R*)-(−)-**5** and (*S*)-(+)-**5**, respectively), the energy gain found for (*R*)-(−)-**5** with respect to (*S*)-(+)-**5** ($\Delta E = -2.82$ kcal/mol) was superior to that calculated for (*S*)-(−)-octoclothepin with respect to its (*R*)-(+)-enantiomer ($\Delta E = -1.09$ kcal/mol). Our calculated ΔE values correlate to the corresponding D_2 receptor affinities of the two pairs of enantiomers; indeed, a relative affinity of 9 between octoclothepin enantiomers corresponds to a conformational energy difference of 1.3 kcal/mol, while a relative affinity of 24 between **5** enantiomers corresponds to a conformational energy difference of about 2 kcal/mol.

To explain the different conformational behavior of (±)-**5** and (±)-octoclothepin enantiomers, we investigated the different capability of (±)-**5** and (±)-octoclothepin enantiomers for reaching their proposed D_2 bioactive conformation. Proposed bioactive folding of the tricyclic system of (*S*)-(−)-octoclothepin and (*R*)-(−)-**5** are

shown in Figure 7 and Table 8 (conformers D and B′, respectively). When the tricyclic system adopts this folding, the α angle value (as defined in Figure 6) is 127° and corresponds to the pyrrole C−N−H external bond angle. Consequently, (*R*)-(−)-**5** bioactive folding is the most stable among (±)-**5** conformers characterized by the piperazine ring in the equatorial position, despite unfavorable steric interactions occurring between piperazine and seven-membered ring hydrogens. The proposed bioactive folding of the tricyclic system of (*R*)-(+)-octoclothepin and (*S*)-(+)-**5** (conformers C and C′ in Table 8 and Figure 7) possesses an α angle value of 119° for (*R*)-(+)-octoclothepin and 122° for (*S*)-(+)-**5**. Consequently, while conformer C represents the most stable "equatorial" conformer of (*R*)-(+)-octoclothepin, with no unfavorable steric contacts (Figure 8, part IV), conformer C′ is the most unstable among (±)-**5** conformers, with an α angle value that induces a steric tension in the pyrrole ring geometry, causing the van der Waals radii overlap shown in Figure 8 (part III vs part IV). Moreover, while the superimposition of the bioactive conformation of (*R*)-(−)-**5** with the one of the corresponding octoclothepin (*S*)-(−)-enantiomer shows a very good structural fit (heavy atoms rmsd value of 0.12 Å, Figure 8, part I), the same superimposition applied to (*S*)-(+)-**5** and (*R*)-(+)-octoclothepin indicates a more pronounced structural difference (heavy atoms rmsd value of 0.30 Å, Figure 8, part II), consistent with the greater difference in their D_2 receptor affinity.

Conclusions

In summary, we have pharmacologically characterized the new, potential atypical antipsychotic (*S*)-(+)-**5** (ST1460). Its receptor affinity profile suggests a possible complex interaction on the cortical receptors involved in the regulation of the activity of prefrontal cortical cells innervated by the VTA neurons, such as 5-HT$_{2A}$, dopaminergic, and α-adrenergic receptor subtypes. The 5-HT$_{2A}$/D$_2$ ratio (expressed by the log $Y = 4.7$) is particularly favorable, and preliminary in vivo studies confirmed pharmacological effects similar to those of olanzapine and superior to those of clozapine in the 5-OMe-DMT-induced head twitches and apomorphine-induced climbing animal models. (*S*)-(+)-**5** has little propensity to induce catalepsy and does not significantly elevate prolactin serum level. These results, taken together, suggest that this compound represents a new, potent atypical antipsychotic, and it has been selected for further pharmacological studies. The (*S*)-(+)-**5** unsubstituted counterpart (±)-**6a** was resynthesized, and its (+)-enantiomer was characterized as an atypical antipsychotic. Starting from (*S*)-(+)-**5** as the lead compound, a series of analogues were developed. Representative compounds are the fluoro analogues (±)-, (+)-, and (−)-**6b** and (±)-**6f,g**, the bromo analogues (±)-**6h−j**, and the chloro-substituted derivatives **6c−e**. Among the described compounds, while the bromo analogue **6h** presented a typical binding profile already in the racemate form, the fluoro analogue (±)-**6b** showed an atypical binding profile (log $Y \approx 5$) and its (+)-enantiomer ((+)-**6b**), together with (*S*)-(+)-**5** and (+)-**6a** (ST1622), represents a new potential atypical antipsychotic drug. Molecular modeling studies identified several structural and conformational features responsible for the binding profile of the described compounds and
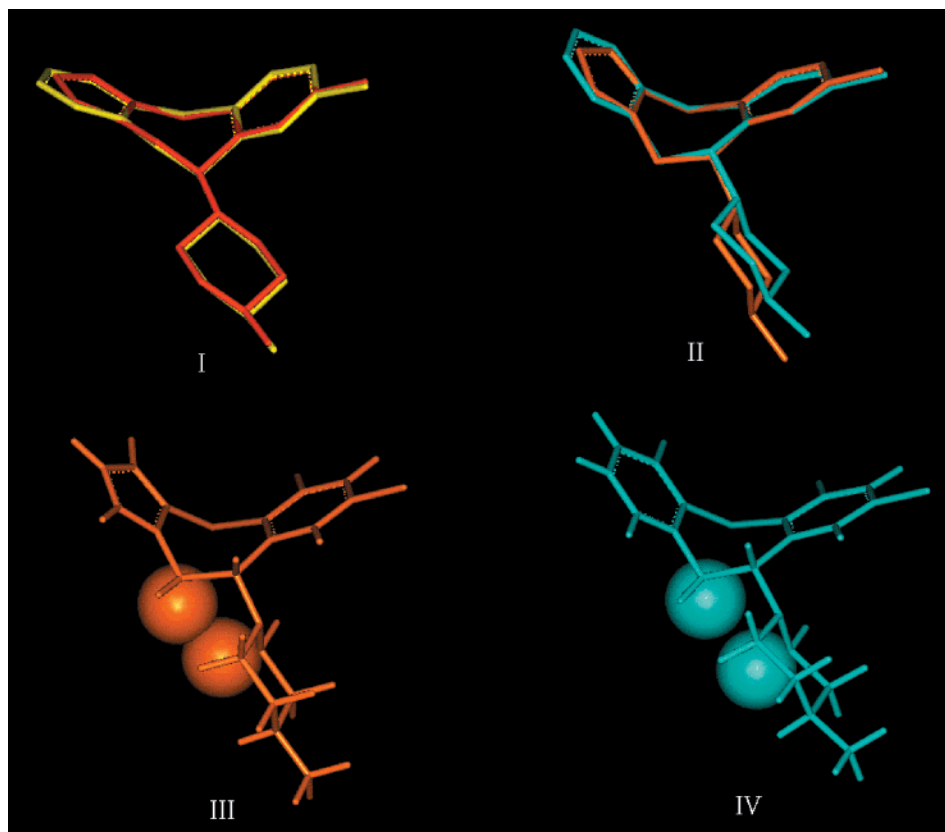
Figure 8. Upper: superimposition by the four aromatic atoms of the seven-membered ring of (I) (*R*)-(−)-**5** (red) with (*S*)-(−)-octoclothepin (yellow) and (II) (*S*)-(+)-**5** (orange) with (*R*)-(+)-octoclothepin (cyan). Lower: comparison of unfavorable steric interactions occurring in (III) (*S*)-(+)-**5** conformer C′ (orange) and (IV) (*R*)-(+)-octoclothepin conformer C (cyan). The van der Waals volumes of the closest hydrogens are displayed.

will lead, in the future, to novel atypical antipsychotics characterized by stereoselective interaction at D_2 receptors.

Experimental Section

Melting points were determined using an Electrothermal 8103 apparatus and are uncorrected. IR spectra were taken with Perkin-Elmer 398 and FT 1600 spectrophotometers. ^{1}H NMR spectra were recorded on Bruker 200 MHz and Varian 500 MHz spectrometers with TMS as internal standard; the value of chemical shifts (δ) are given in ppm and coupling constants (J) in hertz (Hz). All reactions were carried out in an argon atmosphere. GC−MS were performed on a Saturn 3 (Varian) or Saturn 2000 (Varian) GC−MS system using a Chrompack DB5 capillary column (30 m × 0.25 mm i.d.; 0.25 μm film thickness). Mass spectra were recorded using a VG 70-250S spectrometer. HPLC separation was performed using a Chiralpack AD amylose column (097-702-40808) (length × diameter = 250 mm × 10 mm). Elemental analyses were performed on a Perkin-Elmer 240C elemental analyzer, and the results were within ±0.4% of the theoretical values unless otherwise noted. Yields refer to purified products and are not optimized.

5-Bromo-2-methylthiobenzoic Acid (8). To a cooled (0−5 °C) stirring solution of 2-amino-5-bromobenzoic acid **7** (1 g, 4.63 mmol), sodium hydroxide (0.185 g, 4.63 mmol), and sodium nitrite (0.32 g, 4.63 mmol) in water (7.71 mL), a solution of concentrated hydrochloric acid (1.44 mL) in water (2.5 mL) was slowly added. The resulting mixture was stirred at 0−5 °C for 1 h, then was neutralized with potassium carbonate and potassium acetate. The cold diazonium salt solution was run into a vigorously stirred solution of potassium ethylxantate (2.23 g, 13.89 mmol) and water (7.7 mL) previously heated to 75−80 °C; this temperature was maintained during addition and for a further 1 h. Then the reaction

mixture was cooled to room temperature and stirred for 1 h. After that time hydrogen peroxide (3.22 mL) was added and the solution was stirred for 1 night at room temperature. The mixture was filtered, and the solution was acidified (on an ice bath) and filtered again. The crude product, collected as a yellow amorphous solid, was dissolved in water and sodium hydroxide and reprecipitated with hydrochloric acid to afford pure bis(2-hydroxycarbonyl-4-bromophenyl) disulfide (1.02 g) (95% yield), which was directly used in the next step without further purification.

To a solution of bis(2-hydroxycarbonyl-4-bromophenyl) disulfide (1.02 g, 2.15 mmol) in 85% ethanol (17.2 mL) and sodium hydroxide, sodium borohydride (0.163 g) was added in portions. The resulting solution was stirred for 30 min at room temperature and for an additional 3 h at reflux. Then ice was added and the mixture was stirred for 15 min at room temperature. After that time a solution of sodium hydroxide (0.30 g, 7.55 mmol) in water (1.9 mL) and dimethyl sulfate (376 μL, 3.97 mmol) were added and the reaction mixture was stirred for 2.5 h at reflux. After the solution was cooled, 1 drop of 30% ammonium hydroxide (to destroy the excess of dimethyl sulfate) and hydrochloric acid were added until pH 3 was attained. The solid obtained was collected by filtration. The crude product was chromatographed (4% formic acid, 20% ethyl acetate in toluene) to afford 1.017 g of **8** as a yellow solid (96% yield). ^{1}H NMR (DMSO): δ 7.95 (d, 1H, J = 2.7 Hz), 7.70 (dd, 1H, J = 8.8, 1.9 Hz), 7.27 (d, 1H, J = 8.8 Hz), 2.37 (s, 3H). Anal. ($C_8H_7BrO_2S$) C, H.

1-[5-Fluoro-2-(methylthio)phenyl]ethanone (9a). A mixture of 1-fluoro-4-(methylthio)benzene (4.0 g, 28.13 mmol), anhydrous aluminum chloride (8.4 g, 63.0 mmol), and carbon disulfide (89 mL) was heated at reflux under argon atmosphere, and acetic anhydride (2.65 mL, 28.1 mmol) was added dropwise over 2 h. After being refluxed for 24 h, the solution was poured into crushed ice−water (62.5 mL) and concentrated hydrochloric acid (2.7 mL). The organic phase was separated

and water extracted with dichloromethane (3×30 mL), and the combined organic layers were washed with brine, dried, and concentrated. The oily residue was chromatographed (50% petroleum ether, 40–60 °C, in dichloromethane) to afford **9a** (2.98 g) as colorless prisms: mp 82–84 °C (58% yield). ^{1}H NMR (CDCl$_3$): δ 7.45 (dd, 1H, $J = 9.2$, 2.4 Hz), 7.29–7.11 (m, 2H), 2.57 (s, 3H), 2.39 (s, 3H). Anal. (C$_9$H$_9$FOS) C, H.

1-[5-Bromo-2-(methylthio)phenyl]ethanone (9b). A stirred solution of **8** (0.1 g, 0.4 mmol) in dry tetrahydrofuran (3.0 mL) was cooled to 0 °C (ice bath) and treated with methyllithium (1.4 M solution in ether, 1.16 mL, 1.62 mmol). After 2 h at 0 °C under stirring, chlorotrimethylsilane (1.0 mL, 8.1 mmol) was rapidly added while stirring continued, the ice bath was removed, and the reaction mixture was allowed to warm to room temperature. Then 1 N hydrochloric acid (3.0 mL) was added and the resulting two-phase system was stirred at room temperature for 30 min. The organic phase was separated, water was extracted with ether (3×5 mL), and the combined extracts were dried and evaporated. The crude product was chromatographed (30% petroleum ether, 40–60 °C, in dichloromethane) to afford 64 mg of **9b** as a yellowish solid: mp 71–73 °C (64% yield). ^{1}H NMR (CDCl$_3$): δ 7.88 (d, 1H, $J = 1.9$ Hz), 7.55 (dd, 1H, $J = 8.4$, 2.5 Hz), 7.18–7.14 (d, 1H, $J = 8.5$ Hz), 2.58 (s, 3H), 2.39 (s, 3H). Anal. (C$_9$H$_9$BrOS) C, H.

2-Bromo-1-[5-fluoro-2-(methylthio)phenyl]ethanone (10a). To a stirring solution of (**9a**) (2.07 g, 11.3 mmol), carbon tetrachloride (62 mL) and glacial acetic acid (2.0 mL) was added, at room temperature, a solution of bromine (546 μL, 10.7 mmol) in carbon tetrachloride (34 mL). The first drop was added, and after 20 min the solution was added dropwise over 4 h. After the solution was stirred for 16 h, the solvent was distilled and to the residue was added water and solid sodium bicarbonate (to pH 7). The organic phase was separated and water extracted with dichloromethane (3×30 mL), and the organic layers were dried and evaporated. The crude product was chromatographed (70% petroleum ether, 40–60 °C, in dichloromethane) to give 1.9 g of **10a** as a yellowish solid (64% yield). ^{1}H NMR (CDCl$_3$): δ 7.44 (dd, 1H, $J = 8.8$, 2.8 Hz), 7.38–7.18 (m, 2H), 4.42 (s, 2H), 2.43 (s, 3H). Anal. (C$_9$H$_8$ BrFOS) C, H.

2-Bromo-1-[5-bromo-2-(methylthio)phenyl]ethanone (10b). Starting from **9b** (0.6 g, 2.43 mmol), the desired product **10b** was obtained following the procedure described for **10a**. The crude product was chromatographed (50% petroleum ether, 40–60 °C, in dichloromethane) to give 0.57 g (72% yield) of the pure product. ^{1}H NMR (CDCl$_3$): δ 7.87 (d, 1H, $J = 1.6$ Hz), 7.44 (dd, 1H, $J = 8.0$, 2.1), 7.12 (d, 1H, $J = 8.0$ Hz), 4.43 (s, 2H), 2.43 (s, 3H). Anal. (C$_9$H$_8$ Br$_2$OS) C, H.

1-[5-Fluoro-2-(methylthio)phenyl]-2-(pyrrol-1-yl)ethanone (11a). To a stirring solution of hexamethylenetetramine (3.18 g, 22.7 mmol) in chloroform (29.6 mL) a solution of **10a** (1.9 g, 7.2 mmol) in chloroform (16 mL) was added dropwise over 5 min at room temperature. As soon as the 1-[5-fluoro-2-(methylthio)phenyl]ethanone-2-hexaminium bromide was formed, the suspension was rapidly filtered and the desired product was collected as a yellow amorphous solid that was washed with chloroform, dried, and used for the following reaction (99% yield). A suspension of the hexaminium bromide (2.87 g, 7.13 mmol) in methanol (23.6 mL) was cooled to 0 °C, and concentrated hydrochloric acid (3.30 mL) was added. The mixture was stirred for 96 h in the dark at room temperature. The white solid (ammonium chloride) was removed by filtration, and the obtained solution was evaporated. The residue was recrystallized from ethanol to give 2-amino-1-[5-fluoro-2-(methylthio)phenyl]ethanone hydrochloride as a yellow solid that was used in the next step without further purification (yield 98%). To a solution of the amine hydrochloride (2.49 g, 6.98 mmol) in water (15.9 mL), heated at 90 °C, were added sodium acetate trihydrate (0.95 g, 6.98 mmol), glacial acetic acid (9.22 mL), and 2,5-dimethoxytetrahydrofuran (1.31 mL, 10.15 mmol). After 20 s at 90–100 °C the mixture was cooled and extracted with ethyl acetate. The organic layers were washed with a 20% solution of sodium bicarbonate and brine,

dried, and evaporated. The residue was chromatographed (50% petroleum ether, 40–60 °C, in dichloromethane) to afford 0.87 g of (**11a**) as white crystals: mp 133.2–134.0 °C (50% yield). ^{1}H NMR (CDCl$_3$): δ 7.39–7.15 (m, 3H), 6.66 (m, 2H), 6.22 (m, 2H), 5.20 (s, 2H), 2.42 (s, 3H). MS m/z: 252 (M$^+$), 234, 202 (100), 183, 169, 154, 141, 126, 109, 80. Anal. (C$_{13}$H$_{12}$FNOS) C, H, N.

1-[5-Bromo-2-(methylthio)phenyl]-2-(pyrrol-1-yl)ethanone (11b). Starting from **10b** (0.77 g, 5.50 mmol), the desired product was obtained, following the above-described procedure for **11a**, as white crystals: mp 138.0–139.2 °C (32% yield). ^{1}H NMR (CDCl$_3$): δ 7.65 (d, 1H, $J = 1.9$ Hz), 7.58 (dd, 1H, $J = 8.4$, 2.2 Hz), 7.23 (d, 1H, $J = 8.8$ Hz), 6.65 (m, 2H), 6.22 (m, 2H), 5.20 (s, 2H), 2.41 (s, 3H). Anal. (C$_{13}$H$_{12}$BrNOS) C, H, N.

1-[5-Fluoro-2-(methylsulfinyl)phenyl]-2-(pyrrol-1-yl)-ethanone (12a). To a stirred cooled solution of **11a** (1.76 g, 7.06 mmol) in dichloromethane (12 mL) was added dropwise over 30 min a solution of m-chloroperbenzoic acid (71.5% grade, 1.70 g, 7.06 mmol) in dichloromethane (10 mL). After being stirred for 45 min at 0 °C, the mixture was treated with a 5% solution of sodium carbonate in water (41 mL) and was stirred for 15 min at room temperature. The organic phase was separated, and water was extracted with dichloromethane (3×10 mL). The organic layers were dried and evaporated, and the residue was chromatographed (10% dichloromethane in ethyl acetate) to afford 1.02 g of **12a** as white crystals that darkened rapidly (64% yeld). ^{1}H NMR (CDCl$_3$): δ 8.42–8.35 (m, 1H), 7.61–7.51 (m, 2H), 6.68 (m, 2H), 6.26 (m, 2H), 5.28 (q, 2H, $J = 17.9$ Hz), 2.77 (s, 3H). Anal. (C$_{13}$H$_{12}$FNO$_2$S) C, H, N.

1-[5-Bromo-2-(methylsulfinyl)phenyl]-2-(pyrrol-1-yl)-ethanone (12b). Starting from **11b** (0.77 g, 5.5 mmol), the desired product was obtained, following the above-described procedure for **12a**, as colorless prisms: mp 138–139 °C (75% yield). ^{1}H NMR (CDCl$_3$): δ 8.30–8.25 (m, 1H), 8.00 (m, 2H), 6.64 (m, 2H), 6.25 (m, 2H), 5.29 (q, 2H, $J = 17.9$ Hz), 2.77 (s, 3H). Anal. (C$_{13}$H$_{12}$BrNO$_2$S) C, H, N.

7-Fluoro-9,10-dihydropyrrolo[2,1-*b*][1,3]benzothiazepin-9-one (13a). Trifluoroacetic anhydride (1.0 mL) was added dropwise under argon atmosphere to freshly distilled *N,N*-dimethylformamide (8 mL) cooled to 0 °C. After being stirred for 20 min at 0 °C, a solution of **12a** (109 mg, 4.12 mmol) in *N,N*-dimethylformamide (29 mL) was added. After 15 min at room temperature, water (41 mL) was added to the dark-yellow solution and the pH was adjusted to 7 with sodium acetate. The mixture obtained was stirred at room temperature for 1 night. Extraction with dichloromethane, drying of the extracts, and subsequent evaporation of the solvent gave an oily residue, which was chromatographed (30% petroleum ether, 40–60 °C, in dichloromethane). The compound **13a** was recrystallized from *n*-hexane as yellowish crystals: mp 133–134 °C (20% yield). ^{1}H NMR (CDCl$_3$): δ 7.82–7.76 (m, 1H), 7.50 (m, 1H), 7.18 (m, 1H), 6.88 (m, 1H), 6.42 (m, 1H), 6.10 (m, 1H), 5.14 (s, 2H). MS m/z: 233 (100, M$^+$), 205, 200, 172, 126. Anal. (C$_{12}$H$_8$-FNOS) C, H, N.

7-Bromo-9,10-dihydropyrrolo[2,1-*b*][1,3]benzothiazepin-9-one (13b). Method A. According to the procedure described for **13a**, the reaction to obtain **13b** was carried out using trifluoroacetic acid as solvent (0.63 mL) and adding **12b** (0.20 g, 0.62 mmol) to the cold (0 °C) mixture of trifluoroacetic acid and trifluoroacetic anhydride. The desired product **13b** was obtained as yellowish prisms (64% yield).

Method B. To a cold (about 15 °C) solution of **12b** (60 mg, 0.19 mmol) in acetonitrile (1.65 mL), trifluoroacetic anhydride (80 μL, 0.12 g, 0.58 mmol) was added dropwise under argon atmosphere. After 20 min, the starting material was consumed, so we added distilled methanol (0.28 mL) and tetramethylammonium iodide (0.12 g, 0.58 mmol). The resulting mixture was stirred at room temperature for 30 min. Then after evaporation of the solvents, the residue was directly chromatographed (30% petroleum ether, 40–60 °C, in dichloromethane) (69% yield). ^{1}H NMR (CDCl$_3$): δ 8.22 (d, 1H, $J = 1.9$ Hz), 7.53 (dd, 1H, $J = 8.3$, 2.2 Hz), 7.42 (d, 1H, $J = 8.4$ Hz), 6.87 (m, 1H), 6.43 (m, 1H), 6.12 (m, 1H), 5.13 (s, 2H). MS

m/z: 293 (M$^+$, 100), 265, 261, 232, 214, 186, 154, 115. Anal. (C$_{12}$H$_8$BrNOS) C, H, N.

(±)-7-Fluoro-9,10-dihydro-9-hydroxypyrrolo[2,1-*b*][1,3]-benzothiazepine (14a). To a solution of **13a** (37 mg, 0.16 mmol) in dry tetrahydrofuran (0.5 mL) and dry methanol (0.7 mL), cooled to 0 °C under argon atmosphere, sodium borohydride (90 mg, 0.16 mmol) was added in portions. After the mixture was stirred for 1 h at 0 °C, the reaction was quenched with a saturated solution of ammonium chloride (1 mL), the solvent was removed, and the mixture was extracted with ethyl acetate (3 × 2 mL). Combined organic layers were dried over sodium sulfate, filtered, and evaporated, and the crude product was chromatographed (30% petroleum ether, 40−60 °C, in dichloromethane) to give **14a** (36 mg, 96% yield). ^{1}H NMR (CDCl$_3$): δ 7.40 (m, 1H), 7.22 (m, 1H), 6.90 (m, 2H), 6.3 (m, 1H), 6.11 (m, 1H), 5.06 (m, 1H), 4.90 (dd, 1H, *J* = 14.2, 2.2 Hz), 4.30 (dd, 1H, *J* = 14.0, 6.5 Hz), 2.07 (d, 1H, *J* = 9.8 Hz). Anal. (C$_{12}$H$_{10}$FNOS) C, H, N.

(±)-7-Bromo-9,10-dihydro-9-hydroxypyrrolo[2,1-*b*][1,3]-benzothiazepine (14b). Starting from **13b** (0.12 g, 0.39 mmol), the desired product was obtained according to the procedure described for **14a** (65% yield). ^{1}H NMR (CDCl$_3$): δ 7.63 (d, 1H, *J* = 1.7 Hz), 7.32−7.21 (m, 2H), 6.88 (m, 1H), 6.34 (m, 1H), 6.10 (m, 1H), 5.02 (br s, 1H), 4.86 (dd, 1H, *J* = 3.8, 1.8 Hz), 4.32 (dd, 1H, *J* = 14.2, 6.3 Hz), 1.99 (s, 1H). Anal. (C$_{12}$H$_{10}$BrNOS) C, H, N.

(±)-9-Bromo-9,10-dihydro-7-fluoropyrrolo[2,1-*b*][1,3]-benzothiazepine (15a). To a solution of **14a** (0.17 g, 0.71 mmol) in dry ethyl ether (3 mL) a solution of phosphorus tribromide (33.5 μL, 0.36 mmol) in dry ethyl ether (0.7 mL) was added dropwise. The reaction mixture was refluxed for 2 h under argon atmosphere. After the mixture was cooled to room temperature, dry ethanol (143 μL) was added and the resulting solution was heated at reflux for 1 h. Then a total of 4 mL of aqueous sodium carbonate was added; the organic phase was separated, dried, and evaporated. The crude product was chromatographed (50% petroleum ether, 40−60 °C, in dichloromethane) to give 0.103 g of pure **15a** (48% yield). ^{1}H NMR (CDCl$_3$): δ 7.35−7.16 (m, 2H), 6.92−6.82 (m, 2H), 6.38 (m, 1H), 6.11 (m, 1H), 5.67 (m, 1H), 5.51 (dd, 1H, *J* = 14.6, 2.6 Hz), 4.64 (dd, 1H, *J* = 14.8, 7.0 Hz). Anal. (C$_{12}$H$_9$BrFNS) C, H, N.

(±)-7,9-Dibromo-9,10-dihydropyrrolo[2,1-*b*][1,3]benzo-thiazepine (15b). Starting from **14b** (70 mg, 0.25 mmol), the title compound was obtained following the above-described procedure for **15a** (36% yield). ^{1}H NMR (CDCl$_3$): δ 7.59 (m, 1H), 7.28−7.16 (m, 2H), 6.92−6.91 (m, 1H), 6.39−6.37 (m, 1H), 6.13 (m, 1H), 5.65 (dd, 1H, *J* = 6.9, 2.5 Hz), 5.09 (dd, 1H, *J* = 14.6, 2.3 Hz), 4.66 (dd, 1H, *J* = 14.6, 7.0 Hz). Anal. (C$_{12}$H$_9$-Br$_2$NS) C, H, N.

(±)-9,10-Dihydro-7-fluoro-9-(4-methylpiperazin-1-yl)-pyrrolo[2,1-*b*][1,3]benzothiazepine (6b). A mixture of **15a** (50 mg, 0.18 mmol) and *N*-methylpiperazine (1 mL) was heated at 140 °C for 17 h under argon atmosphere. The reaction mixture was then cooled, diluted with ethyl acetate (30 mL), and washed with brine. Combined organic layers were dried over sodium sulfate, filtered, and evaporated; the oily residue was chromatographed (10% triethylamine in ethyl acetate) to afford 37 mg of **6b** as a colorless solid: mp 213−214 °C (63% yield). ^{1}H NMR (CDCl$_3$): δ 7.37−7.26 (m, 2H), 6.85−6.76 (m, 2H), 6.29 (m, 1H), 6.06 (m, 1H), 4.78−4.67 (m, 1H), 4.45 (dd, 1H, *J* = 14.2, 3.5 Hz), 3.96 (dd, 1H, *J* = 8.9, 3.3 Hz), 2.64−2.37 (m, 8H), 2.25 (s, 3H). MS *m/z*: 318 (100, M$^+$), 277, 218, 185. Anal. (C$_{17}$H$_{20}$FN$_3$S) C, H, N.

(±)-7-Chloro-9,10-dihydro-9-(4-ethylpiperazin-1-yl)pyr-rolo[2,1-*b*][1,3]benzothiazepine (6c). To a cold (0 °C) solution of **16b** (0.19 g, 0.56 mmol) in glacial acetic acid (4.09 mL), sodium borohydride (0.31 g, 8.18 mmol) was added in portions. The resulting mixture was stirred at room temperature overnight. Then water and sodium bicarbonate were added until pH 7 was attained. The water phase was extracted with dichloromethane (3 × 25 mL). Combined organic layers were dried over sodium sulfate, filtered, and evaporated. After purification (flash chromatography, 20% methanol in ethyl acetate) we obtained **6c** (84% yield) as colorless crystals. ^{1}H NMR (CDCl$_3$): δ 7.51 (d, 1H, *J* = 2.1 Hz), 7.33 (d, 1H, *J* = 8.2 Hz), 7.06 (dd, 1H, *J* = 8.3, 2.3 Hz), 6.8 (m, 1H), 6.30 (m, 1H), 6.07 (m, 1H), 4.68 (dd, 1H, *J* = 14.1, 8.7 Hz), 4.52 (dd, 1H, *J* = 14.0, 3.6 Hz), 3.96 (dd, 1H, *J* = 8.6, 3.4 Hz), 2.60−2.40 (m, 10H), 1.10 (t, 3H, *J* = 7.3 Hz). Anal. (C$_{18}$H$_{22}$ClN$_3$S) C, H, N.

(±)-7-Chloro-9,10-dihydro-9-[4-(2′-hydroxy)ethylpiper-azin-1-yl]pyrrolo-[2,1-*b*][1,3]benzothiazepine (6d). A solution of **15c** (0.10 g, 0.32 mmol), β-hydroxyethylpiperazine (87 μL, 0.32 mmol), and 2-butanone (3 mL) was refluxed for 21 h. The reaction mixture was then evaporated, and water was added to the residue. The resulting water phase was extracted with ethyl acetate, and combined extracts were dried, filtered, and evaporated. The crude product was chromatographed (10% methanol in ethyl acetate) to give **6d** as a colorless oil (82% yield). ^{1}H NMR (CDCl$_3$): δ 7.30 (d, 1H, *J* = 8.5 Hz), 7.07 (dd, 1H, *J* = 8.4, 2.0 Hz), 7.50 (m, 1H), 6.86 (m, 1H), 6.30 (m, 1H), 6.07 (m, 1H), 4.70 (dd, 1H, *J* = 13.9, 8.8 Hz), 4.51 (dd, 1H, *J* = 14.0, 3.5 Hz), 3.93 (dd, 1H, *J* = 8.6, 3.2 Hz), 3.60 (t, 2H, *J* = 5.3 Hz), 2.56−2.46 (m, 10H). MS *m/z*: 364 (M$^+$, 100), 333, 284, 234, 201, 143, 129, 100, 70, 56. Anal. (C$_{18}$H$_{22}$ClN$_3$OS) C, H, N.

(±)-7-Chloro-9,10-dihydro-9-(4-methylhexahydro-1*H*-1,4-diazepin-1-yl)pyrrolo-[2,1-*b*][1,3]benzothiazepine (6e). The title compound was obtained according to the procedure reported for **6c**, starting from **16a** (0.02 g, 0.05 mmol) (59% yield). ^{1}H NMR (CDCl$_3$): δ 7.63 (d, 1H, *J* = 2.0 Hz), 7.26 (d, 1H, *J* = 8.2 Hz), 7.03 (dd, 1H, *J* = 8.2, 2.5 Hz), 6.83 (m, 1H), 6.27 (m, 1H), 6.03 (m, 1H), 4.83 (dd, 1H, *J* = 14.2, 8.6 Hz), 4.45 (dd, 1H, *J* = 14.4, 3.0 Hz), 4.00 (dd, 1H, *J* = 8.6, 2.9 Hz), 2.84−2.60 (m, 8H), 2.33 (s, 3H), 1.78−1.70 (m, 2H). MS *m/z*: 347 (M$^+$, 100), 276, 267, 234, 220, 127, 113, 84, 70, 56. Anal. (C$_{18}$H$_{22}$ClN$_3$S) C, H, N.

(±)-9,10-Dihydro-9-(4-ethylpiperazin-1-yl)-7-fluoropyr-rolo[2,1-*b*][1,3]benzothiazepine (6f). The desired product **6f** was obtained starting from **15a** (53 mg, 0.178 mmol), using 4-ethylpiperazine (1 mL) and following the above-described procedure for **6b**. The colorless oil **6f** was obtained in 73% yield. ^{1}H NMR (CDCl$_3$): δ 7.37−7.26 (m, 2H), 6.86−6.75 (m, 2H), 6.26 (m, 1H), 6.05 (m, 1H), 4.80−4.68 (m, 1H), 4.39 (dd, 1H, *J* = 13.9, 3.7 Hz), 3.97 (dd, 1H, *J* = 9.2, 3.6 Hz), 2.60−2.32 (m, 10H), 1.08 (t, 3H, *J* = 7.3 Hz). MS *m/z*: 332 (M$^+$, 100), 277, 218, 185, 115. Anal. (C$_{18}$H$_{22}$FN$_3$S) C, H, N.

(±)-9,10-Dihydro-7-fluoro-9-[4-(2′-hydroxy)ethylpiper-azin-1-yl]pyrrolo[2,1-*b*][1,3]benzothiazepine (6g). According to the procedure described for **6d**, starting from **15a** (65 mg, 0.218 mmol), the desired product **6g** was obtained as a colorless amorphous solid (69% yield). ^{1}H NMR (CDCl$_3$): δ 7.37−7.24 (m, 2H), 6.86−6.77 (m, 2H), 6.29 (m, 1H), 6.06 (m, 1H), 4.72 (m, 1H), 4.40 (dd, 1H, *J* = 14.1, 3.4 Hz), 3.96 (dd, 1H, *J* = 8.9, 3.5 Hz), 3.59 (t, 2H, *J* = 5.3 Hz), 2.85 (br s, 1H), 2.57−2.47 (m, 10H). MS *m/z*: 348 (M$^+$, 100), 288, 218, 185. Anal. (C$_{18}$H$_{22}$FN$_3$OS) C, H, N.

(±)-7-Bromo-9,10-dihydro-9-(4-methylpiperazin-1-yl)-pyrrolo[2,1-*b*][1,3]benzothiazepine (6h). Starting from **16c** (0.114 g, 0.303 mmol) and following the procedure reported for **6c**, after chromatographic purification (20% methanol in ethyl acetate) we obtained 91 mg (79% yield) of the desired product as a colorless amorphous solid. ^{1}H NMR (CDCl$_3$): δ 7.64 (s, 1H), 7.35−7.21 (m, 2H), 6.86 (m, 1H), 6.29 (m, 1H), 6.06 (m, 1H), 4.73−4.61 (m, 1H), 4.45 (dd, 1H, *J* = 14.3, 8.5 Hz), 3.98 (dd, 1H, *J* = 8.6, 3.5 Hz), 2.57−2.37 (m, 11H). MS *m/z*: 378 (M$^+$, 100), 297, 280, 247, 199, 167, 113 (100), 99, 70, 56. Anal. (C$_{17}$H$_{20}$BrN$_3$S) C, H, N.

(±)-7-Bromo-9,10-dihydro-9-(4-ethylpiperazin-1-yl)pyr-rolo[2,1-*b*][1,3]benzothiazepine (6i). The title compound was obtained starting from **16d** (0.135 g, 0.346 mmol) following the above-described procedure for **6c**. Compound **6i** was obtained in 76% yield (0.049 g). ^{1}H NMR (CDCl$_3$): δ 7.64 (s, 1H), 7.22 (m, 2H), 6.86 (m, 1H), 6.29 (m, 1H), 6.04 (m, 1H), 4.70 (dd, 1H, *J* = 14.0, 8.8 Hz), 4.49 (dd, 1H, *J* = 14.1, 3.6 Hz), 3.96 (dd, 1H, *J* = 8.9, 3.5 Hz), 2.57−2.33 (m, 10H), 1.08

(t, 3H, $J = 7.2$ Hz). MS *m/z*: 393 (M$^+$), 313, 280, 247, 199, 167, 127 (100), 113, 84, 70, 56. Anal. (C$_{18}$H$_{22}$BrN$_3$S) C, H, N.

(±)-7-Bromo-9,10-dihydro-9-[4-(2′-hydroxy)ethylpiperazin-1-yl]pyrrolo[2,1-*b*][1,3]benzothiazepine (6j). The title compound was obtained following the procedure described for **6d**. Starting from **15b** (0.197 g, 0.549 mmol), the desired product was obtained as a yellowish oil, 49 mg, (22% yield). ^{1}H NMR (CDCl$_3$): δ 7.62 (m, 1H), 7.23 (m, 2H), 6.87 (m, 1H), 6.30–6.28 (m, 1H), 6.08–6.04 (m, 1H), 4.68–4.61 (m, 1H), 4.50–4.41 (dd, 1H, $J = 14.2, 3.4$ Hz), 3.99–3.93 (dd, 1H, $J = 8.5, 3.5$ Hz), 3.68–3.63 (t, 2H, $J = 5.0$ Hz), 2.65–2.41 (m, 11H). MS *m/z*: 407 (M$^+$ + H), 374, 328, 278, 246, 199, 167, 143 (100), 129, 100, 56. Anal. (C$_{18}$H$_{22}$BrN$_3$OS) C, H, N.

7-Chloro-9-(4-methylhexahydro-1*H*-1,4-diazepin-1-yl)-pyrrolo[2,1-*b*][1,3]benzothiazepine (16a). A solution of **13c** (30 mg, 0.12 mmol), 1-methylhomopiperazine (0.06 mL, 5.41 mmol), and trimethylsilyl triflate (58 μL, 0.07 g, 0.33 mmol) was heated at 120 °C with stirring. After a few minutes, 0.06 mL of 1-methylhomopiperazine was added and the reaction was kept at 120 °C for 3 h. After that time water was added and the reaction mixture was extracted with dichloromethane. The organic layer was dried over sodium sulfate, filtered, and evaporated to give the crude product that was purified by means of flash chromatography (20% methanol in ethyl acetate) to afford the pure title compound with a yield of 41%. ^{1}H NMR (CDCl$_3$): δ 7.53 (d, 1H, $J = 2.4$ Hz), 7.45 (d, 1H, $J = 8.7$ Hz), 7.25 (dd, 1H, $J = 8.4, 2.4$ Hz), 6.75 (m, 1H), 6.55 (s, 1H), 6.19 (m, 1H), 6.11 (m, 1H), 3.23–3.15 (m, 4H), 3.15–2.61 (m, 4H), 2.40 (s, 3H), 1.95 (m, 2H). MS *m/z*: 345 (100, M$^+$), 205, 140, 97. Anal. (C$_{18}$H$_{20}$ClN$_3$S) C, H, N.

7-Chloro-9-(4-ethylpiperazin-1-yl)pyrrolo[2,1-*b*][1,3]-benzothiazepine (16b). Starting from **13c** (0.19 g, 0.76 mmol), *N*-ethylpiperazine (0.70 mL, 6.13 mmol), and trimethylsilyl triflate (0.37 mL, 0.46 g, 2.09 mmol), compound **16b** was synthesized following the procedure described for **16a** (74% yield). ^{1}H NMR (CDCl$_3$): δ 7.62 (d, 1H, $J = 1.9$ Hz), 7.43 (d, 1H, $J = 8.0$ Hz), 7.23 (d, 1H, $J = 8.0$ Hz), 6.75 (m, 1H), 6.57 (s, 1H), 6.22–6.15 (m, 1H), 6.10 (m, 1H), 2.91 (m, 4H), 2.58–2.42 (m, 6H), 1.10 (t, 3H, $J = 7.1$ Hz). Anal. (C$_{18}$H$_{20}$ClN$_3$S) C, H, N.

7-Bromo-9-(4-methylpiperazin-1-yl)pyrrolo[2,1-*b*][1,3]benzothiazepine (16c). Starting from **13b** (0.10 g, 0.34 mmol), *N*-methylpiperazine (0.169 mL, 1.53 mmol), and trimethylsilyl triflate (0.17 mL, 0.93 mmol), the title compound was obtained as for **16a** (84% yield). ^{1}H NMR (CDCl$_3$): δ 7.76 (m, 1H), 7.37 (m, 2H), 6.75–6.70 (m, 1H), 6.57 (m, 1H), 6.22 (m, 1H), 6.11 (m, 1H), 2.89–2.80 (m, 4H), 2.56–2.45 (m, 4H), 2.35 (s, 3H). Anal. (C$_{17}$H$_{18}$BrN$_3$S) C, H, N.

7-Bromo-9-(4-ethylpiperazin-1-yl)pyrrolo[2,1-*b*][1,3]-benzothiazepine (16d). The title compound was obtained following the above-described procedure for **16c**, starting from **13b** (0.10 g, 0.34 mmol), *N*-ethylpiperazine (0.169 mL, 1.53 mmol), and trimethylsilyl triflate (0.17 mL, 0.93 mmol). Then 0.50 mL of *N*-ethylpiperazine was added. After purification 0.125 g of the desired pure product was obtained as a white solid (94% yield). ^{1}H NMR (CDCl$_3$): δ 7.76 (m, 1H), 7.36 (m, 1 H), 7.25 (m, 1 H), 6.75 (m, 1H), 6.57 (m, 1H), 6.22 (m, 1H), 6.10 (m, 1H), 2.90 (m, 4H), 2.60–2.46 (m, 6H), 1.12 (t, 3H, $J = 7.0$ Hz). MS *m/z*: 390 (M$^+$), 356, 137, 111, 97, 84 (100), 69, 57. Anal. (C$_{18}$H$_{20}$BrN$_3$S) C, H, N.

Olanzapine 4. A sample of this antipsychotic agent has been obtained following the procedure as described in ref 13. The structure was confirmed by ^{1}H NMR and MS.

X-ray Crystallography. Single crystals of (−)-**5** tartrate were obtained by dissolving equimolar amounts of (−)-**5** and enantiomerically pure (*S,S*)-tartaric acid in methanol and allowing the solution to become concentrated at room temperature.

A colorless single crystal of (−)-**5** tartrate (C$_{21}$H$_{26}$N$_3$SClO$_6$·H$_2$O, MW = 502.0) of approximate dimensions 0.10 mm × 0.25 mm × 0.15 mm was submitted to X-ray data collection on a Siemens P4 four-circle diffractometer with graphite monochromated Mo Kα radiation (λ = 0.710 69 Å). Lattice parameters were determined by least-squares refinement on 41 randomly selected and automatically centered reflections. The $ω-2θ$ scan technique was used in the data collection in the $4° \le 2θ \le 50°$ scan range. The parameters were the following: crystal system, orthorhombic; space group, *P*2$_1$2$_1$2$_1$; $a = 9.192$-(2) Å, $b = 9.834(1)$ Å, $c = 26.165(4)$ Å; $V = 2365.3(8)$ Å^3; $Z = 4$, $D_c = 1.410$ g/cm^3. A total of 4751 reflections were collected at 22 °C of which 4134 are unique ($R_{int} = 0.11$). Absorption correction obtained by ψ scans was applied. Full crystal details are reported in Table 1 of Supporting Information.

The structure was solved by direct methods implemented in the SHELX-97 program.[33] The refinement was carried out by full-matrix anisotropic least-squares on F^2 for all reflections for non-H atoms by using the SHELX-97 program.[33] The absolute configuration of the chiral center at the benzothiazepine nucleus was made by selecting the diastereoisomer having the known (*S,S*) configuration of the tartaric acid. In this diastereoisomer the configuration of the unknown chiral center is *R*. The refined Flack parameter was 0.4(3).[34]

The final refinement converged to R1 = 0.109, wR2 = 0.086 for $I > 2\ σ(I)$, goodness-of-fit = 0.97. Minimum and maximum height in the last Δρ map was −0.25 and 0.25 e Å^{-3}, respectively.

In Vitro Binding Assays.[15] 1. Serotonin and Dopamine Receptors. Male CRL:CD(SD)BR-COBS rats (Charles River, Italy) were killed by decapitation. Their brains were rapidly dissected into the various areas (striatum for D$_1$ and D$_2$ receptors, olfactory tubercle for D$_3$ receptors, and cortex for 5-HT$_2$ receptors) and stored at −80 °C until the day of assay. Tissues were homogenized in about 50 volumes of ice-cold 50 mM Tris-HCl, pH 7.4 (for D$_1$, D$_2$, and 5-HT$_2$ receptors) or 50 mM Hepes Na, pH 7.5 (for D$_3$ receptors) using an Ultra-Turrax TP-1810 homogenizer (2 × 20 s) and centrifuged at 48 000g for 10 min (Beckman Avanti J-25 centrifuge). Each pellet was resuspended in the same volume of fresh buffer, incubated at 37 °C for 10 min, and centrifuged again at 48 000g for 10 min. The pellet was then washed once by resuspension in fresh buffer and centrifuged as before. The pellets obtained were resuspended in the appropriate incubation buffer (50 mM Tris-HCl, pH 7.4, containing 10 μM pargyline, 0.1% ascorbic acid, 120 mM NaCl, 5 mM KCl, 2 mM CaCl$_2$, and 1 mM MgCl$_2$ for D$_1$ and D$_2$ receptors; 50 mM Hepes Na, pH 7.5, containing 1 mM EDTA, 0.005% ascorbic acid, 0.1% albumin, and 200 nM eliprodil for D$_3$ receptors; 50 mM Tris-HCl, pH 7.7, for 5-HT$_2$ receptors) just before the binding assay. [^{3}H]SCH 23390 (specific activity, 71.1 Ci/mmol; NEN) binding to D$_1$ receptors was assayed in a final incubation volume of 0.5 mL consisting of 0.25 mL of membrane suspension (2 mg of tissue/sample), 0.25 mL of [^{3}H]ligand (0.4 nM), and 10 μL of displacing agent or solvent. Nonspecific binding was obtained in the presence of 10 μM (−)-*cis*-flupentixol.

[^{3}H]Spiperone (specific activity, 16.5 Ci/mmol; NEN) binding to D$_2$ receptors was assayed in a final incubation volume of 1 mL consisting of 0.5 mL of membrane suspension (1 mg of tissue/sample), 0.5 mL of [^{3}H]ligand (0.2 nM), and 20 μL of displacing agent or solvent. Nonspecific binding was obtained in the presence of 100 μM (−)-sulpiride.

[^{3}H]-7OH-DPAT (specific activity, 159 Ci/mmol; Amersham) binding to D$_3$ receptors was assayed in a final incubation volume of 1 mL consisting of 0.5 mL of membrane suspension (10 mg of tissue/sample), 0.5 mL of [^{3}H]ligand (0.7 nM), and 20 μL of displacing agent or solvent. Nonspecific binding was obtained in the presence of 1 μM dopamine.

[^{3}H]Ketanserin (specific activity, 63.3 Ci/mmol; Amersham) binding to 5-HT$_2$ receptors was assayed in a final incubation volume of 1 mL consisting of 0.5 mL of membrane suspension (5 mg of tissue/sample), 0.5 mL of [^{3}H]ligand (0.7 nM), and 20 μL of displacing agent or solvent. Nonspecific binding was obtained in the presence of 1 μM methisergide.

Incubations (15 min at 37 °C for D$_1$, D$_2$, and 5-HT$_2$ receptors, 60 min at 25 °C for D$_3$ receptors) were stopped by rapid filtration under vacuum through GF/B (for D$_1$, D$_2$, and 5-HT$_2$ receptors) or GF/C (for D$_3$ receptors) filters, which were then washed with 12 mL (4 × 3 times) of ice-cold buffer (50 mM Tris-HCl, pH 7.7) using a Brandel M-48R cell harvester. The

radioactivity trapped on the filters was counted in 4 mL of Ultima Gold MV (Packard) in a LKB 1214 rack β liquid scintillation spectrometer with a counting efficiency of 50%.

Dose−inhibition curves were analyzed by the "Allfit" [35] program to obtain the concentration of unlabeled drug that caused 50% inhibition of ligand binding. The K_i values were derived from the IC_{50} values according to the method of Cheng and Prusoff.[36]

2. H$_1$ Histamine Receptor. Binding was determined using membranes prepared from rat cerebral cortex. The cerebral cortex was homogenized in phosphate buffer. The homogenate was centrifuged at $48\,000g$ for 10 min. The pellet was suspended in phosphate buffer and washed twice more. A total of 500 μL of this homogenate was incubated with 500 μL of 1 nM [^{3}H]Pyrilamine and 20 μL of test compound for 60 min at 30 °C and then filtered through a Whatman GF/B filter (Whatman International, Ltd.). Radioactivity on the filter was measured with a liquid scintillation counter. Complete (100%) inhibition of [^{3}H]Pyrilamine binding was determined in the presence of 1 μM promethazine.

3. Acetylcholine Muscarinic Receptors. Binding was determined using membranes prepared from rat cerebral cortex. The cerebral cortex was homogenized in phosphate buffer. The homogenate was centrifuged at $48\,000g$ for 10 min. The pellet was suspended in phosphate buffer and washed twice more. A total of 1 mL of this homogenate was incubated with 1 mL of 0.16 nM [^{3}H]QNB (quinuclidinyl benzilate, L-[benzilic-4,4'-3H]-) and 40 μL of test compound for 60 min at 37 °C and then filtered through a Whatman GF/B filter (Whatman International, Ltd.). Radioactivity on the filter was measured with a liquid scintillation counter. Complete (100%) inhibition of [^{3}H]QNB binding was determined in the presence of 1 μM atropine.

4. α_1 Adrenergic Receptors. Binding was determined using membranes prepared from rat cerebral cortex. The cerebral cortex was homogenized in phosphate buffer. The homogenate was centrifugated at $44\,000g$ for 10 min. The pellet was suspended in phosphate buffer and washed twice more. A total of 500 μL of this homogenate was incubated with 500 μL of 0.2 nM [^{3}H]Prazosin and 20 μL of test compound for 30 min at 25 °C and then filtered through a Whatman GF/B filter (Whatman International, Ltd.). Radioactivity on the filter was measured with a liquid scintillation counter. Complete (100%) inhibition of [^{3}H]Prazosin binding was determined in the presence of 10 μM prazosin.

5. α_2 Adrenergic Receptors. Binding was determined using membranes prepared from rat cerebral cortex. The cerebral cortex was homogenized in phosphate buffer. The homogenate was centrifugated at $44\,000g$ for 10 min. The pellet was suspended in phosphate buffer and washed twice more. A total of 500 μL of this homogenate was incubated with 500 μL of 1 nM [^{3}H]Clonidine and 20 μL of test compound for 30 min at 25 °C and then filtered through a Whatman GF/B filter (Whatman International, Ltd.). Radioactivity on the filter was measured with a liquid scintillation counter. Complete (100%) inhibition of [^{3}H]Clonidine binding was determined in the presence of 10 μM clonidine.

Behavioral Test. 1. Antagonism of Apomorphine-Induced Climbing in Mouse. Male albino mice CD1, weighing 20−25 g at the beginning of the studies, were used. Mice exhibited wall climbing behavior following the subcutaneous administration of apomorphine (1.3 mg/kg). To quantify this behavior, the animals were placed individually in upturned, steel cylinders (height, 18 cm; diameter, 14 cm) with walls of vertical bars (diameter, 2 mm; 1 cm apart).

Animals given control saline injections remained on the floor of their individual cylinders, exhibiting normal exploratory behavior, while animals receiving apomorphine climbed up the walls of the cylinders holding the wire mesh with their four paws. During a period of climbing, animals did not remain in one position but moved constantly around the sides or the tops of the cages, holding onto the wire mesh with their four paws.[37]

The test compound or vehicle was administrated by the subcutaneous or oral route 30 or 60 min, respectively, before

apomorphine treatment. Climbing behavior was assessed in the animals at 5 min intervals for 30 min, starting 5 min after apomorphine treatment.

2. Antagonism of 5-MeO-DMT-Induced Head Twitches in Mouse. Groups of 10 mice of the CD1 (male strain) were utilized to evaluate head twitches induced by 5-methoxy-*N,N*-dimethyltryptamine (5-MeO-DMT) at a subcutaneous dosage of 10 mg/kg. The evaluations were begun 6 min from the 5-MeO-DMT treatment and lasted after 15 min (counting the number of head twitches produced by the animal). The substances were administered subcutaneously or orally 30 or 60 min, respectively, before the 5-MeO-DMT treatment.[38]

3. Induction of Catalepsy. The test was performed on male Wistar rats (seven to eight animals per group). The procedure employed was similar to that described by Moore[39] with minor changes. The catalepsy evaluation was carried out by means of a metallic bar 0.6 cm in diameter positioned 10 cm above the tabletop. The test consisted of positioning the animal with its forepaws on the bar and timing how long the animal remained hanging onto the bar, employing an end point of 60 s with the criterion of "all or none" being used.

The substances under study were administered by subcutaneous route 30 min before the first evaluation. The subsequent observations were recorded at 60, 90, 120, 180, 240, and 300 min from the administration of compounds.

Calculation. ED_{50} values were calculated by sigmoidal dose−response curve analysis, using the standard statistical package GraphPad Program Prism.

Determination of Serum Prolactin Levels. Fischer 344 rats (275−300 g) were assigned to 5 groups of 10 animals each. The animals were treated with the following compounds: vehicle (2 mL of 0.9% NaCl/kg, sc); haloperidol (2.7 μmol/kg, sc, PM 375.88); olanzapine (12.3 μmol/kg, sc, PM 312.44); clozapine (12.3 μmol/kg, sc, PM 326.83); (*S*)-(+)-**5** (12.3 μmol/kg, sc, PM 406.81).

The rats were killed by decapitation at the following times from treatment: 30, 60, and 180 min. Blood samples (2 mL) were collected, and after centrifugation ($3000g$ for 30 min) the resulting serum samples were stored at −20 °C until analysis for prolactin (PRL). Serum prolactin levels were determined by means of an EIA kit from Amersham.

Microdialysis Experiments. Brain dialysis was performed as previously described.[40a] In brief, male Fischer 344 (Charles River) rats weighing 275−350 g were anesthetised with chloral hydrate anesthesia (400 mg/kg, ip) and placed in a stereotaxic instrument (D. Kopf Instruments). Dialysis tube was inserted transversely through the striatum. Coordinates to the bregma and dura surface (Paxinos and Watson, 1982) were the following: AP, +0.5; V, −4.9. At 24 h after the surgery, the probe was perfused at a flow rate of 2 μL/min with a Ringer solution (147 mM NaCl; 1.5 mM CaCl; 4 mM KCl). Perfusate samples were collected every 30 min into microcentrifuge tubes with 10 μL of perchloric acid (0.2 M). Three consecutive samples were collected at 30 min intervals and served as baseline, then two doses of tested compounds were sequentially administrated to the animals with an interval of 120 min between doses.

Samples were automatically subjected to high-performance liquid chromatography with an electrochemical detection system by an autosample processor (Waters) and analyzed according to the method of Santiago et. al.[40b] to determinate dopamine (DA), dihydroxyphenylacetic acid, (DOPAC), and homovanillic acid (HVA) levels before and after the treatment with tested compounds.

The DA, DOPAC, and HVA levels in each dialysate sample was expressed as a percentage of the average baseline level calculated from the three fractions collected before the first administration of tested compounds. The postinjection changes, with respect to baseline levels, of DA, DOPAC, and HVA were determined by calculating the area under the curve (AUC) after each dose of tested compound (AUC first treatment; AUC second treatment) and were expressed as a percentage of basal values. To evaluate the whole postinjection effect of each

compound, the total area under the curve of sequential treatment with two doses (AUC total) was considered.

Data were analyzed statistically by Student's *t*-test for unpairerd data. Significance is reported at the $p \leq 0.05$ level.

Molecular Modeling. All molecular modeling was run on a Silicon Graphics Indigo2 R10000 workstation. The X-ray structure of *R*-(−)-**5**, determined by us, and the one of *S*-(+)-octoclothepin, extracted from the Cambridge Crystallographic Structural Data Bank, were used as a starting point for subsequent calculations. Systematic conformational searches (SCS) were carried out using the SEARCH routine in Sybyl 6.6 (Tripos, St. Louis. MO). Starting conformations were generated on the basis of the proposed three-dimensional D_2 pharmacophoric model.[16] Torsional angles included in rings were analyzed using the ring search module by increment of 10° using 0−359° as an interval of variation. The permissible variance on the distance between the ring-closure atoms was set to 1 Å, while the permissible variance on the valence angles about the ring-closure atoms was set to 15°. Piperazine rotation was analyzed with an angle (τ_N in Figure 6) increment of 10° within a 0−359° range. To generate all theoretically possible conformations, a 0.05 van der Waals radii scaling factor was used in the rigid rotamers, and no conformational energy evaluation was included in all the searches. Resulting structure files were transferred to the Insight2000 (MSI, San Diego) package to perform energy calculations. Potential energy curves were calculated for each molecule by the scanning of τ and τ_S values (see Figure 6), followed by a full energy minimization, except for the dihedral angle used as driving angle. All the conformations were geometrically optimized (Discover module) using the cvff force field[41] and a distance-dependent dielectric constant ($\epsilon = 80r$). Energy minimizations were performed with conjugate gradient as the minimization algorithm[42] until the maximum rms derivative was less than 0.001 kcal/mol. For each molecule, the obtained torsional angle values were plotted against their conformational energies using the table function in Insight2000. Resulting molecular mechanics minima, as well as (±)-**5** and (±)-octoclothepin enantiomers bioactive conformation, were subjected to a full geometry optimization by semiempirical calculations using the quantum mechanical method PM3 in the Mopac[43] 6.0 package in the Ampac/Mopac module of Insight2000. All PM3 minimizations were carried out using the keyword PRECISE. In the different calculations the molecules were considered with the distal piperazine nitrogen in the protonated state.

Supporting Information Available: Crystal data, atomic coordinates, bond lengths, and bond angles for (*R*)-(−)-**5** (Tables 1−3). This material is available free of charge via the Internet at http://pubs.acs.org.

References

(1) Calne, D. B. *Therapeutics and Neurology*; Blackwell Scientific Publications: Oxford, 1980; p 281.

(2) Carlsson, A. The Current Status of the Dopamine Hypothesis of Schizophrenia. *Neuropsychopharmacology* **1988**, *1*, 179−186.

(3) Meltzer, H. Y. Clinical studies on the mechanism of action of clozapine: the dopamine−serotonin hypothesis of schizophrenia. *Psychopharmacology* **1989**, *99*, S18−S27.

(4) (a) Hertel, P.; Fagerquist, M. V.; Svensson, T. H. Enhanced cortical dopamine output and antipsychotic-like effects of raclopride by α_2 adrenoceptor blockade. *Science* **1999**, *286*, 105−107. (b) Lindström, L. H. Schizophrenia, the dopamine hypothesis and α_2-adrenoceptor antagonists. *Trends Pharmacol. Sci.* **2000**, *21*, 198−199.

(5) Niemegeers, C. J. E.; Awouters, F.; Heylen, S. L. E.; Gelders, Y. G. 5-HT_2 receptor antagonists in schizophrenia: preclinical and clinical considerations. In *Biological Psychiatry*; Racagni, G., Ed.; Elsevier Science Publishers: Amsterdam, 1991; Vol. 1, pp 535−537.

(6) Alvir, J. M.; Lieberman, J. A.; Safferman, A. Z.; Schwimmer, J. L.; Schaaf, J. A. Clozapine-induced agranulocytosis. Incidence and risk factors in United States. *N. Engl. J. Med.* **1993**, *329*, 162.

(7) Honigfield, G.; Arellano, F.; Sethi, J. Reducing clozapine-related morbidity and mortality: 5 years of experience with the Clozaril national registry. *J. Clin. Psychiatry* **1998**, *59*, 3−7.

(8) Worrel, J. A.; Marken, P. A.; Beckman, S. E.; Ruehter, V. L. Atypical antipsychotic agents: A critical review. *Am. J. Health-Syst. Pharm.* **2000**, *57*, S37−S50.

(9) Elliott Richelson, M. D. Receptor pharmacology of neuroleptics: relation to clinical effects. *J. Clin. Psychiatry* **1999**, *60*, 5−14.

(10) (a) Bymaster, F.; Perry, K. W.; Nelson, D. L.; Wong, D. T.; Rasmussen, K.; Moore, N. A.; Calligaro, D. O. Olanzapine: a basic science update. *Br. J. Psychiatry* **1999**, *174*, 36−40. (b) Fulton, B.; Goa, K. L. Olanzapine—A review of its pharmacological properties and therapeutic efficacy in the management of schizophrenia and related psychosis. *Drugs* **1997**, *53* (2), 281−298. (c) Beasley, C. M.; Tollefson, G. D.; Tran, P. V. Safety of olanzapine. *J. Clin. Psychiatry* **1997**, *58*, 13−17. (d) Gómez, J. C.; Sacristán, J. A.; Hernández, J.; Breier, A.; Carrasco, P. Z.; Saiz, C. A.; Fontova Carbonell, E. The safety of olanzapine compared with other antipsychotic drugs: results of an observational prospective study in patients with schizophrenia (EFESO study). *J. Clin. Psychiatry* **2000**, *61* (5), 335−343.

(11) Moore, N. A.; Calligaro, D. O.; Wong, D. T.; Bymaster, F.; Tye, N. C. The pharmacology of olanzapine and other new antipsychotic agents. *Curr. Opin. Invest. Drugs* **1993**, *2* (4), 281−293.

(12) Naumann, R.; Falbe, W.; Heilemann, H.; Reuster, T. Olanzapine-induced agranulocytosis. *Lancet* **1999**, *354*, 566−567.

(13) Gardner, I.; Leeder, J. S.; Chin, T.; Zahid, N.; Uetrecht, W. A comparison of covalent binding of clozapine and olanzapine to human neutrophils in vitro and in vivo. *Mol. Pharmacol.* **1998**, *53*, 999−1008.

(14) Gardner, I.; Zahid, N.; McCrimmon, D.; Uetrecht, J. P. Comparison of the oxidation of clozapine and olanzapine to reactive metabolites and the toxicity of these metabolites to human leucocytes. *Mol. Pharmacol.* **1998**, *53*, 991−998.

(15) Campiani, G.; Nacci, V.; Bechelli, S.; Ciani, S.; Garofalo, A.; Fiorini, I.; Wikstrom, H.; de Boer, P.; Tepper, P. G.; Cagnotto, A.; Mennini, T. New antipsychotic agents with serotonin and dopamine antagonist properties based on a pyrrolo[2,1-*b*][1,3]-benzothiazepine structure. *J. Med. Chem.* **1998**, *41*, 3763−3772.

(16) (a) Liljefors, T.; Bøgesø, K. P. Conformational analysis and structural comparisons of (1*R*,3*S*)-(+)- and (1*S*,3*R*)-(−)-tefludazine, (*S*)-(+)- and (*R*)-(−)-octoclothepin, and (+)-dexclamol in relation to dopamine receptor antagonism and amine-uptake inhibition. *J. Med. Chem.* **1988**, *31*, 306−312. (b) Bøgesø, K. P.; Liljefors, T.; Arnt, J.; Hyttel, J.; Pedersen, H. Octoclothepin enantiomers. A reinvestigation of their biochemical and pharmacological activity in relation to a new receptor-interaction model for dopamine D_2 receptor antagonists. *J. Med. Chem.* **1991**, *34*, 2023−2030.

(17) Villa, L.; Ferri, V.; Grana, E.; Cattarini Mastelli, O.; Sossi, D. Sintesi e proprietá farmacologiche di *n*-isopropilfeniletanolammine orto-, meta- o para sostituite. *Farmaco, Ed. Sci.* **1969**, *24*, 329−340.

(18) Henry, R. A.; Hollins, R. A.; Lowe-Ma, C.; Moore, D. W.; Nissan, R. A. Anomalous reaction of pentafluorophenacyl bromide with examethylenetetramine. structure of the product. *J. Org. Chem.* **1990**, *55*, 1796−1801.

(19) Artico, M.; Corelli, F.; Massa, S.; Stefanich, G. A Facile and Convenient Synthesis of the Unknown 1-Aroylmethyl-1*H*-pyrroles. *Synthesis* **1983**, 931.

(20) (a) Garofalo, A.; Campiani, G.; Nacci, V.; Fiorini, I. Polycondensed heterocycles. VIII. Synthesis of 11-aryl-5H,11H-pyrrolo-[2,1-*c*][1,4]benzothiazepines by Pummerer rearrangement−cyclization reaction. *Heterocycles* **1992**, *34*, 51−59. (b) Bates, D. K.; Winters, R. T.; Picard, J. A. Interrupted Pummerer rearrangement: capture of tricoordinate sulfur species generated under Pummerer rearrangement conditions. *J. Org. Chem.* **1992**, *57*, 3094−3097.

(21) Campiani, G.; Nacci, V.; Corelli, F.; Anzini, M. Polycondensed heterocycles. VII. A convenient synthesis of pyrrolo[1,2-*a*]quinoxaline derivatives by intramolecular aromatic nucleophilic displacement. *Synth. Commun.* **1991**, *21*, 1567−1576.

(22) Meltzer, H. Y.; Matsubara, S.; Lee, J.-C. Classification of typical and atypical antipsychotic drugs on the basis of dopamine D-1, D-2 and serotonin₂ pki values. *J. Pharmacol. Exp. Ther.* **1989**, *251*, 238−246.

(23) Lieberman, J. A.; Mailman, R. B.; Buncan, G.; Sikich, L.; Chakos, M.; Nichols, D. E.; Kraus, J. E. A decade of serotonin research: role of serotonin in treatment of psychosis. Serotoninergic basis of antipsychotic drug effects in schizophrenia. *Biol. Psychiatry* **1998**, *44*, 1099−1117.

(24) Abi-dargham, A.; Laruelle, M.; Charney, D.; Krystal, J. The role of serotonin in pathophisiology and treatment of schizophrenia. *J. Neuropsychiatry* **1997**, *9*, 1−17.

(25) Saller, C. F.; Czupryna, M. J.; Salama, A. I. 5-HT$_2$ receptor blockade by ICI 169,369 and other 5-HT$_2$ antagonists modulate the effects of D$_2$ dopamine receptor blockade. *J. Pharmacol. Exp. Ther.* **1991**, *253*, 1162−1170.

(26) Lucas, G.; De Deurwardére, P.; Caccia, S.; Spampinato, U. The effect of serotonergic agents on haloperidol-induced striatal dopamine release in vivo: opposite role of 5-HT$_{2A}$ and 5-HT$_{2C}$ receptor subtypes and significance of the haloperidol dose used. *Neuropharmacology* **2000**, *39*, 1053−1063.

(27) Lucas, G.; De Deurwardére, P.; Porras, G.; Spampinato, U. Endogenous serotonin enhances the release of dopamine in the striatum only when nigro-striatal dopaminergic transmission is activated. *Neuropharmacology* **2000**, *39*, 1984−1995.

(28) De Deurwardére, P.; Spampinato, U. Role of serotonin 2B\2C receptor subtypes in the control of accumbal and striatal dopamine release elicited in vivo by dorsal raphe nucleus electrical stimulation. *J. Neurochem.* **1999**, *73* (2), 1033−1042.

(29) Di Giovanni, G.; De Deurwardére, P.; Di Mascio, M.; Di Matteo, V.; Esposito, E.; Spampinato, U. Selective blockade of serotonin-2C\2B receptors enhances mesolimbic and mesostriatal dopaminergic function: a combined in vivo electrophysiological and microdialysis study. *Neuroscience* **1999**, *91* (2), 587−597.

(30) Lucas, G.; Spampinato, U. Role of striatal serotonin 2A and serotonin 2C receptor subtypes in the control of in vivo dopamine outflow in the rat striatum. *J. Neurochem.* **2000**, *74*, 693−701.

(31) Gudelsky, G. A.; Koening, J. I.; Simonovic, M.; Koiama, T.; Ohmori, T.; Meltzer, H. Y. Differential effects of Haloperidol, Clozapine and Fluperlapine on tuberoinfundibular dopamine neurons and prolactin secretion in the rat. *J. Neural. Transm.* **1987**, *68,* 227−240.

(32) Froimowitz, M.; Rämsby, S. Conformational properties of semi-rigid antipsychotic drugs: the pharmacophore for dopamine D-2 antagonist activity. *J. Med. Chem.* **1991**, *34*, 1707−1714.

(33) Sheldrick, G. M. *SHELX-97*, release 97-2; University of Göttingen, Göttingen, Germany, 1997.

(34) Flack, H. D. *Acta Crystallogr.* **1983**, *A39*, 876−881.

(35) De Lean, K. W.; Munson, P. J.; Rodbard, D. Simultaneous analysis of families of sigmoidal curves: application to bioassay, radioligand assay and physiological dose−response curves. *Am. J. Physiol.* **1978**, *235*, E97−E102.

(36) Cheng, Y.; Prusoff, W. H. Relationship between the inhibition costant (Ki) and the concentration of inhibition which causes 50% inhibition (IC$_{50}$) of an enzymatic reaction. *Biochem. Pharmacol.* **1973**, *22*, 3099−3108.

(37) Costall, B.; Naylor, R. J.; Nohria, V. Climbing behaviour induced by apomorphine in mice: a potential model for detection of neuroleptic activity. *Eur. J. Pharmacol.* **1978**, *50*, 39−50.

(38) Rigdon, G. C.; Norman, M. H.; Cooper, B. B.; Howard, J. L.; Boncek, V. M.; Faison, W. L.; Nanry, K. P.; Pollard, G. T. 1192U90 in animal tests that predict antipsychotic efficacy, anxiolysis, and extrapyramidal side effects. *Neuropsychopharmacology* **1996**, *15*, 231−242.

(39) Moore, N. A.; Tye, N. C.; Axton, M. S.; Risius, F. C. The behavioral pharmacology of olanzapine, a novel "atypical" antipsychotic agent. *J. Pharmacol. Exp. Ther.* **1992**, *262*, 545−551.

(40) (a) Di Chiara, G.; Imperato, A. Rapid tolerance to neuroleptic-induced stimulation of dopamine release in freely moving rats. *J. Pharmacol. Exp. Ther.* **1985**, *235*, 487−494. (b) Santiago, M.; Machado, A.; Cano, J. Effects of age and dopamine agonist and antagonist on striatal dopamine release in the rat, an in vivo microdyalisis study. *Mech. Ageing Dev.* **1993**, *67*, 261−267.

(41) Dauber-Osguthorpe, P.; Roberts, V. A.; Osguthorpe, D. J.; Wolff, J.; Genest, M.; Hagler, A. T. Structure and energetics of ligand binding to proteins. *Proteins: Struct., Funct., Genet.* **1988**, *4*, 31−47.

(42) Fletcher, R. Unconstrained Optimization. In *Pratical Methods of Optimization*; John Wiley & Sons: New York, 1980; Vol. 1.

(43) Stewart, J. J. P. MOPAC: A Semiempirical Molecular Orbital Program *J. Comput.-Aided Mol. Des.* **1990**, *4*, 1−105.